*Encyclopedia of Polymer Sceince and Technology*
Copyright © 2005 John Wiley & Sons, Inc. All rights reserved.

# POLYMER BLENDS

## Polymer Blends

Mixing of two or more different polymers together makes it possible to achieve various property combinations of the final material—usually in a more cost-effective way than in the case of synthesis of new polymers. Therefore, great attention has been paid to the investigation of these systems, as well as to the development of specific materials. Recently, the problem of polymer blends has also become important for recycling industrial and/or municipal plastics scrap. A considerable amount of information has been collected during more than three decades, summarized in dozens of monographs (see General References).

Basic problems associated with the equilibrium and interfacial behavior of polymers, compatibilization of immiscible components, phase structure development, and the methods of its investigation are described herein. Special attention is paid to mechanical properties of heterogeneous blends and their prediction. Commercially important types of polymer blends as well as the recycling of commingled plastic waste are briefly discussed.

## Equilibrium Phase Behavior

Mixing of two amorphous polymers can produce either a homogeneous mixture at the molecular level or a heterogeneous phase-separated blend. Demixing of polymer chains produces two totally separated phases, and hence leads to macrophase separation in polymer blends. Some specific types of organized structures may be formed in block copolymers due to microphase separation of block chains within one block copolymer molecule.

Two terms for blends are commonly used in literature—miscible blend and compatible blend. The terminology recommended by Utracki (1) will be used in this article. By the *miscible polymer blend*, we mean a blend of two or more amorphous polymers homogeneous down to the molecular level and fulfilling the thermodynamic conditions for a miscible multicomponent system. An *immiscible polymer blend* is the blend that does not comply with the thermodynamic conditions of phase stability. The term *compatible polymer blend* indicates a commercially attractive polymer mixture that is visibly homogeneous, frequently with improved physical properties compared with the constituent polymers.

## 2 POLYMER BLENDS

Equilibrium phase behavior of polymer blends complies with the general thermodynamic rules (2–6)

$$\Delta G_{\text{mix}} = \Delta H_{\text{mix}} - T\Delta S_{\text{mix}} < 0 \tag{1}$$

and

$$\mu_i^{'} = \mu_i^{''}\ i = 1,2,\ldots,n \tag{2}$$

where $\Delta G_{\text{mix}}$, $\Delta H_{\text{mix}}$, and $\Delta S_{\text{mix}}$ are the Gibbs energy, enthalpy, and entropy of mixing of a system consisting of $i$ components, respectively, $\mu_{\text{i}}'$ and $\mu_{\text{i}}''$ are the chemical potentials of the component $i$ in the phase $\mu'$ and $\mu''$. The condition given in equation 1 is necessary but it is not sufficient. Equation 2 must be also fulfilled.

Generally for a compressible polymer blend the following requirement must be satisfied (5–7):

$$\left(\frac{\partial^2 \Delta G_{\text{mix}}}{\partial v_i^2}\right)_{T,P} = \left(\frac{\partial^2 \Delta G_{\text{mix}}}{\partial v_i^2}\right)_V + \left(\frac{\partial V}{\partial P}\right)_{T,v_i}\left(\frac{\partial^2 \Delta G_{\text{mix}}}{\partial v_i \partial V}\right) > 0 \tag{3}$$

where $v_i$ is the volume fraction of component $i$, $V$ molar volume of blend, P and T are pressure and temperature of the system. If we consider an incompressible system with $\Delta V_{\text{mix}} = 0$, the application of equation 3 to the simple Flory–Huggins relationship for $\Delta G_{\text{mix}}$ (4) leads to the condition of these stability

$$\frac{1}{N_1 v_1} + \frac{1}{N_2 v_2} - 2\chi_{12} \geq 0 \tag{4}$$

where $N_1$, $N_2$ are the numbers of segments of polymer 1 or 2, and $\chi_{12}$ is the interaction parameter between polymers 1 and 2. The entropy contribution (the first and second terms on the left-hand side of equation 4 supporting miscibility of polymers is practically zero ($N_1, N_2 \gg 1$). In this case, the miscibility is controlled by the enthalpy of mixing (interaction parameter $\chi_{12}$). For nonpolar polymers without strong interactions, the temperature dependence of $\chi_{12}$ (Fig. 1, curve 1) is given as

$$\chi_{12} = A + \frac{B}{T} \tag{5}$$

where $A$ and $B$ are positive constants characterizing enthalpy and entropy parts of interaction parameter $\chi_{12}$, respectively. Its positive value indicates a very poor miscibility of high molecular weight nonpolar polymers.

Relationships describing the compressibility of polymer blends are based on the equations-of-state theories (5,6,8–16). These relationships include contributions to the entropy and enthalpy of mixing resulting from volume changes during mixing. The temperature dependence of free-volume interaction is schematically presented as curve 2 in Fig. 1. This value plays a decisive role in determining phase behavior of a polymer blend at high temperature range.

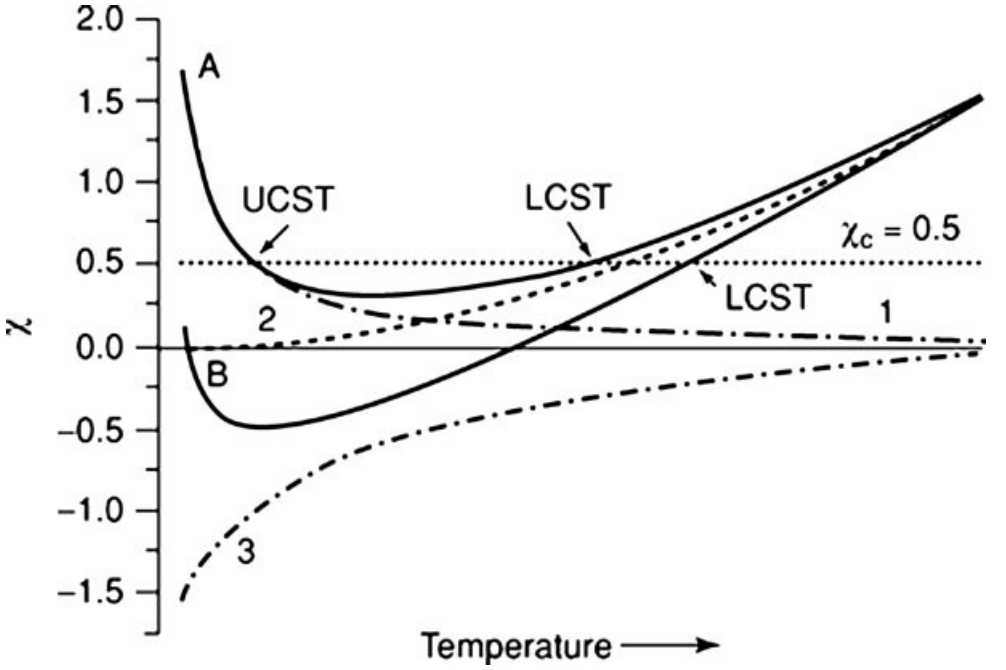


**Fig. 1.** Schematic temperature dependence of interaction parameters resulting from different types of interactions in a polymer blend. (1-dispersive interactions, 2-free-volume interactions, 3-specific interactions, A-sum of 1+2, B-sum of 1+2+3).

From the equation 4 it follows that the negative value of parameter $\chi_{12}$ is necessary to obtain a stable homogeneous polymer blend. The negative value of $\chi_{12}$ is characteristic of systems with specific interactions such as dipole–dipole or hydrogen bond interactions (1,5,6,17). A schematic representation of the temperature dependence of a specific interaction parameter, according (13), is given in Figure 1, curve 3.

The critical value of interaction parameter $\chi_c$ for "symmetric" polymer blends of polymers 1 and 2 ($N_1 = N_2 = N$, $N$-number of segments in polymer chain) is $\chi_c = 2/N$. When $\chi_{12}$ value crosses the critical value, a polymer blend separates into two macrophases. The character of the temperature dependence of $\chi_{12}$ determines the shape of the phase diagram (Fig. 1). Figure 2 shows schematic binodal and spinodal curves corresponding to the different types of interaction parameters presented in Figure 1. Binodal curves (Fig. 2, curves 1–4), defining the two-phase region, are calculated from equation 2 (2,4–6,18). A spinodal curve is obtained by solving of equation 4. The spinodal curve defines the region of absolute instability of the polymer blend. The point common to the binodal and spinodal curves is the critical point. The position of the critical point of a blend of monodisperse polymers coincides with the maximum (UCST-upper critical solution temperature) or minimum (LCST-lower critical solution temperature) of a binodal curve (18) (Fig. 2). If only dispersive interactions among polymer molecules are effective in a blend (Fig. 1, curve 1), partial miscibility can be expected at low temperatures. Above the UCST, the polymer blend is homogeneous (Fig. 2 curve 1) (4–6). Values

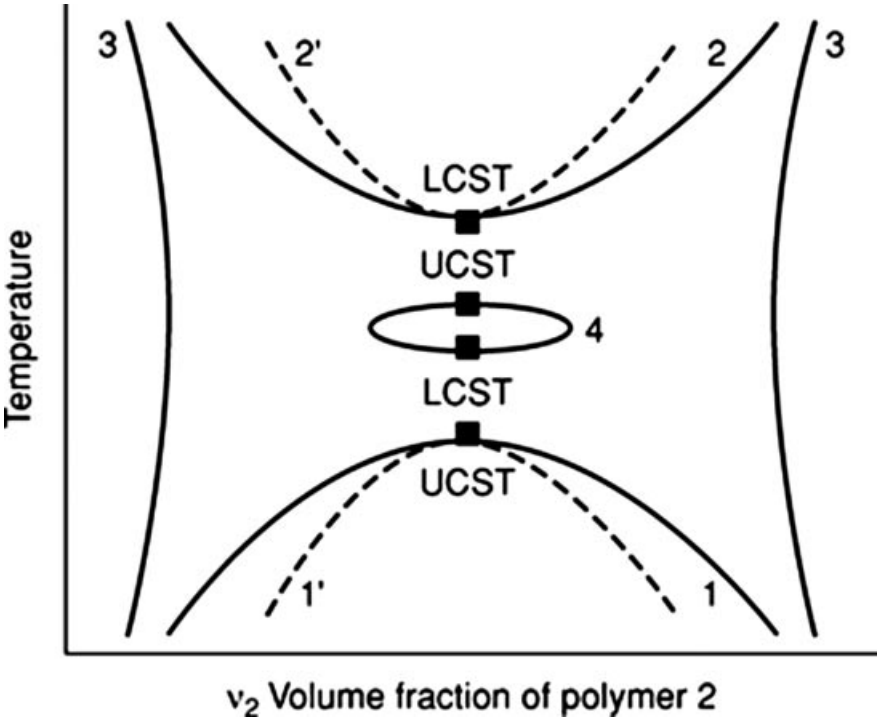


**Fig. 2.** Possible types of phase diagrams corresponding to interactions in Figure 1 (—— ——binodal curves, ———- spinodal curves, UCST—upper critical solution temperature, LCST—lower critical solution temperature).

of interaction parameters of nonpolar polymers can be found in literature (1,5,6) or estimated from the solubility parameters, $\delta_1$ and $\delta_2$, of the neat components

$$\chi \approx (\delta_1 - \delta_2)^2 \tag{6}$$

The $\chi$ parameter of disperse interactions is always positive, and miscibility is driven only by combinatorial entropy of mixing. In general, nonpolar polymers are rarely miscible with each other. Considerable data relevant to interaction energies obtained by different techniques can be found in the literature (5,6,19,20).

The area below the spinodal curve is the region of absolute instability of a polymer blend. The phase separation in this region is controlled by a spinodal mechanism. The region between spinodal and binodal curves is called the metastable region. Phase separation in this region is controlled by a nucleation mechanism.

Phase structure at an initial stage of phase decomposition depends on the type of decomposition mechanisms. The characteristic trait of the spinodal decomposition in an absolutely unstable region is phase separation in the whole volume of a blend. Initially, the resulting structure is very fine, but gradually gets coarse (5,21), and the final stage of separation is full macrophase separation. If the phase separation takes place in the metastable region, the decomposition of a blend

depends on the formation of a nucleus of a new phase. The resulting structure at the initial stage is grainy. The critical sizes of existing nuclei increase by Ostwald ripening mechanism (16)—small grains dissolve and large grains grow due to the dependence of the concentration gradient of dissolved molecules of the nucleating component, which are in turn dependent on grain radius. At the final stage, when the separation is finished, the full phase-separated structure is again obtained (5).

In unstable region, appearing fluctuations increase. The fluctuations can be considered as a set of sinusoidal waves with a constant length (6,16). The amplitude of the fluctuations appearing in the initial stage of the phase separation increases with time, as described by Kwei and Wang in Reference 6. The phase structure of the system is co-continuous for a broad range of blend compositions. At the end of the process, separated phases are identical to the blend components. Theories describing various stages of spinodal decomposition (using various approximations) have been developed (16). Scattering methods have been used for many experimental studies of phase structure decomposition in polymer blends. The initial, intermediate, and late stages of phase structure separation, differing in the time dependence of the domain size of individual phases were identified. The individual stages of the phase structure development are described by different time dependences of the phase domain size. The development of spatial concentration fluctuation is generally described by Ginsburg–Landau equation, considering chemical potential as a function of the order parameter, contribution of the random forces, and the hydrodynamic interaction between polymer molecules (16). Similar equations also describe polymer dissolution if, due to a change in thermodynamics parameters, an immiscible blend passes to a miscible one. The phase separation is affected by the presence of a copolymer and by a shear flow (16). A more detailed description of the kinetics of phase decomposition in polymer blends can be found in Reference 16.

If we have a system with free-volume or specific interactions, an increase in temperature causes phase separation at LCST. In real systems, where several types of interactions are effective, phase behavior with two regions of partial miscibility of components with UCST and LCST (Fig. 2, binodals 1 and 2) or hourglass-shaped binodal and spinodal curves (Fig. 2, binodal 3) can be expected (5,6,9,13–16). In some cases, a closed loop of immiscibility with LCST and UCST (Fig. 2, binodal 4) or a closed loop and region of partial immiscibility at high temperatures with LCST (Fig. 2, binodals 2 and 4) are observed. This pattern of phase behavior is caused by a diminishing intensity of specific interactions with increasing temperature.

Whether polymers are miscible or not depends on a delicate balance of interactions among all components in a system (6). Any favorable gain in the energy of mixing is accompanied by an unfavorable noncombinatorial entropy effect (22,23).

The effective value of the interaction parameter $\chi_{\text{eff}}$ of a multicomponent polymer blend is controlled by its composition. Blends containing statistical copolymers of A and B monomers can be used as examples. Using the mean field-theory leads to the following relation for $\chi_{\text{eff}}$

$$\chi_{\text{eff}} = \sum_i \sum_{j>i} \chi_{ij} \left(v_i^{\text{A}} - v_j^{\text{B}}\right)\left(v_i^{\text{B}} - v_j^{\text{A}}\right) \tag{7}$$

where $\chi_{ij}$ is the interaction parameter between segments $i$ and $j$. For the identical type of segments, its value is zero. It follows from equation 7 that at a proper composition of copolymers, the value of $\chi_{ij}$ can be negative, and the resulting blend is homogeneous.

The former discussion deals with liquid–liquid phase behavior; however, one or both components of the blend can sometimes crystallize. For a polymer pair that is miscible in the melt, cooling well below the melting point of pure crystallizable component leads to a pure crystalline phase of that component. Far below the melting point, the free energy of crystallization is considerably larger than that of mixing. Because polymers never become 100% crystalline, the pure crystals coexist with a mixed amorphous phase consisting of the material that did not crystallize (6,7).

The morphology of heterogeneous polymer blends is controlled by interfacial tension. The interfacial tension, $\sigma$, is intrinsically positive and can be defined as the change in the Gibbs free energy when the interfacial area $A$ is reversibly increased at constant temperature and pressure at closed system (24).

$$\sigma = \left(\frac{\partial G}{\partial A}\right)_{T,P} \tag{8}$$

In a multicomponent system, the tendency to minimize the system Gibbs free energy leads to migration of the minor component on the interface. The resulting increase in concentration of this component at the interface (compared to its concentration in the bulk) (24) decreases the interfacial tension, as follows from equation 9

$$\frac{\partial \sigma}{\partial \ln c_2} = -RT\left(\frac{\Delta N_2}{V N_1}\right) \tag{9}$$

where $c_2$ is the molar concentration of the component 2, $\Delta N_2$ is the excess number of molecules of the component 2 on the interface, $N_1$ is the number of molecules of the component 1, and $V$ is volume of the system. Therefore low energy additives can greatly reduce the interfacial tension between polymers, and hence are expected to increase the degree of dispersion in blends. Block and graft copolymers are the most effective interfacial agents. They show considerable surface activity of the low energy components, and their emulsifying property depends on their structure.

## Compatibilization

As it follows from thermodynamics, the blends of immiscible polymers obtained by simple mixing show a strong separation tendency, leading to a coarse structure and low interfacial adhesion. The final material then shows poor mechanical properties. On the other hand, the immiscibility or limited miscibility of polymers enables formation of a wide range structures, some of which, if stabilized, can impart excellent end-use properties to the final material. To obtain such a stabilized structure, it is necessary to ensure a proper phase dispersion by decreasing interfacial tension to suppress phase separation and improve adhesion. This can

be achieved by modification of the interface by the formation of bonds (physical or chemical) between the polymers. This procedure is known as compatibilization, and the active component creating the bonding as the compatibilizer (1,6,7). Two general methods are used for compatibilization of immiscible polymers: (i) incorporation of suitable block or graft copolymers, or (ii) reactive compatibilization.

**Incorporation of Copolymers (Nonreactive Compatibilization).** Block or graft copolymers with segments that are miscible with their respective polymer components show a tendency to be localized at the interface between immiscible blend phases. The copolymers anchor their segments in the relevant polymer, reducing interfacial tension and stabilizing dispersion against coalescence (24–52). Random copolymers, sometimes also used as compatibilizers, reduce interfacial tension, but their ability to stabilize the phase structure is limited (53). Finer morphology and higher adhesion of the blend lead to improved mechanical properties. The morphology of the resulting two-phase (multiphase) material, and consequently its properties, depend on a number of factors, such as copolymer architecture (type, number, and molecular parameters of segments), blend composition, blending conditions, and the like (25,38,39). Creton and co-workers (54) have reviewed the molecular criteria for copolymers linking two immiscible homopolymers that must be fulfilled to achieve a good stress-transfer ability of the interface. In Figure 3, the conformation of different block, graft, or random copolymers at the interface is schematically drawn.

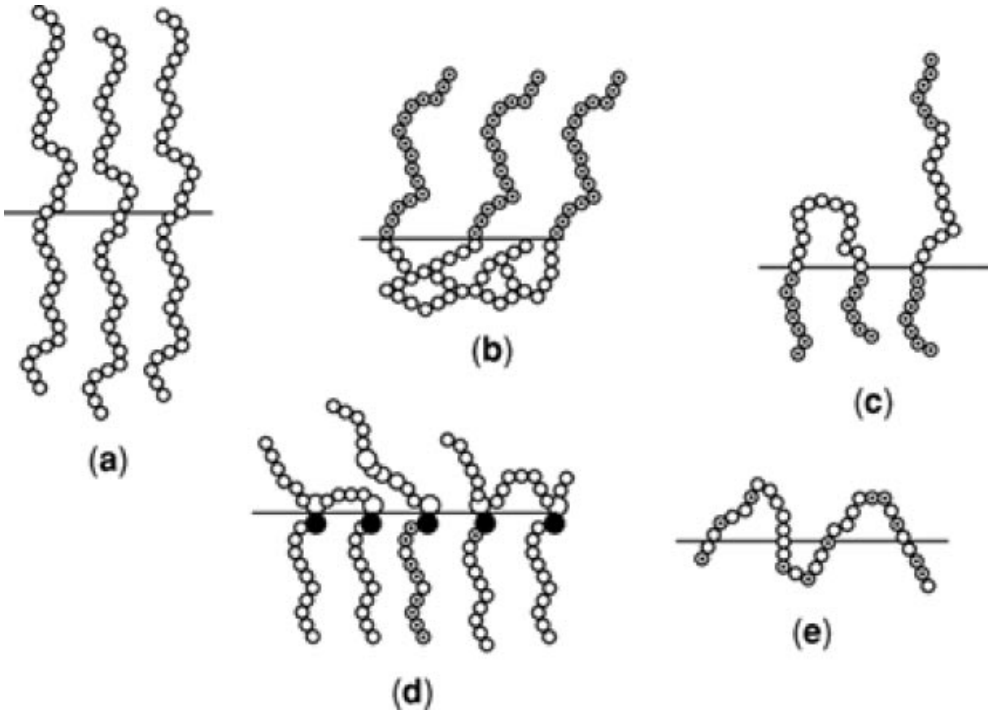


**Fig. 3.** Possible localization of A-B copolymer at the A/B interface. Schematic of connecting chains at an interface, a-diblock copolymers, b-end-grafted chains, c-triblock copolymers,d-multiply grafted chain, and e-random copolymer.

Besides copolymers synthesized specially for compatibilization of immiscible polymers, commercial products (typically used as impact modifiers) are utilized as compatibilizers in research as well as in practice. Typical examples are styrene-butadiene block copolymers and their styrene-hydrogenated butadiene analogues used for compatibilization of styrene polymers (PS, HIPS, SAN, ABS), with polyolefins (49), or ethylene–propylene copolymers for compatibilization of various polyolefins (50).

Mechanical properties that are sensitive to stress transfer (impact strength, tensile strength, elongation) are usually considered as criteria of compatibilization efficiency because they indirectly characterize interface adhesion (1,7,45). Morphological characteristics, such as particle size of the dispersed phase, structure homogeneity, character of interfacial layer, existence of micelles, or mesophases, also give evidence on the compatibilization efficiency (25,29,40–44).

This process, however, inherently bears two practical limitations. Blending of an immiscible polymer pair requires a specific block or graft copolymer. Consequently, a specific synthetic procedure is necessary to obtain the desired copolymer. This can be costly, and sometimes there is no feasible technology at manufacturer's disposal. Moreover, the amount of the copolymer to be added is often significantly higher than that for saturation of the interface. A part of the copolymer may be trapped in the bulk phase during blending and never reach the interface. This fact can negatively affect the blend morphology and may lead to a higher compatibilizer consumption.

During more than three decades, much information on nonreactive compatibilization has been obtained and successfully applied in the development of new multiphase materials. Moreover, the prove efficiency of block or graft copolymers in the controlling of the phase structure development has led to new, more effective approaches to producing these copolymers directly during the blending. This process is known as reactive compatibilization.

**Reactive Compatibilization.** Reactive compatibilization is the process that allows generating graft or block copolymers acting as compatibilizers *in situ* during melt blending (46,55). These copolymers are formed by reactions at the interfaces between suitably functionalized polymers, and they link the immiscible phases by covalent or ionic bonds. In this process, the copolymers are formed directly at the interfaces, where they act like preformed copolymers, ie, they reduce the size of the dispersed phase and improve adhesion. For this reason, the problem with transport of the compatibilizer to interface is not relevant and structure control is easier than in the case of adding preformed copolymers. In order to achieve efficient compatibilization of polymer blends, the reactions between the functional groups should be selective and fast, and the mixing conditions should minimize the limitation of mass transfer in the course of the reaction.

There are several types of reactive compatibilization. If the mixed polymers contain reactive groups, the reaction is straightforward. The polymers without reactive groups have to be functionalized or a miscible polymer containing proper reactive groups is added to the respective component. Therefore, reactive groups such as anhydride, hydroxy, amine, or carboxy are incorporated, into one or both of the polymers to be compatibilized. Maleic anhydride-grafted polymers, such as PP, PE, EPR, EPDM, SEBS, or ABS (46,55), which can react with polymers

containing amino group can serve as examples:

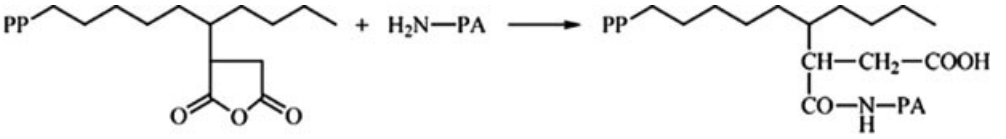


Reactive compatibilization of polymers through copolymer formation is also possible with the help of low molecular weight compounds (56), eg by combination of a peroxide with an oligomer coagent for preparation of PE/PP blends (57) or bis-maleic imide for PE/PBT (58). Special cases of reactive compatibilization can be considered radical-initiated reactions of monomers forming homopolymers and grafts on the chains of dissolved polymers. This process is used for manufacture of such important polymers as HIPS or ABS (59).

## Preparation and Phase Structure Development

**Methods of Blend Preparation.** Most polymer pairs are immiscible, and therefore, their blends are not formed spontaneously. Moreover, the phase structure of polymer blends is not equilibrium and depends on the process of their preparation. Five different methods are used for the preparation of polymer blends (60,61): melt mixing, solution blending, latex mixing, partial block or graft copolymerization, and preparation of interpenetrating polymer networks. It should be mentioned that due to high viscosity of polymer melts, one of these methods is required for size reduction of the components (to the order of $\mu$m), even for miscible blends.

Melt mixing is the most widespread method of polymer blend preparation in practice. The blend components are mixed in the molten state in extruders or batch mixers. Advantages of the method are well-defined components and universality of mixing devices—the same extruders or batch mixers can be used for a wide range of polymer blends. Disadvantages of the method are high energy consumption and possible unfavorable chemical changes of blend components. Evolution of the phase structure in polymer blends during melt mixing and rules for prediction of the structure of the formed phases are discussed in the next section.

During several past years, novel solid state processing methods, such as shear pulverization or cryogenic mechanical alloying, have been developed to provide efficient mixing of polymer blends (62). The polymers are disintegrated in pulverizers at cryogenic temperatures, and nanoscale blend morphologies are achieved. Since the blends are prepared as solid powders, they must be consequently processed in the melt for concrete manufacture. Mechanochemistry of this process makes it possible to obtain block or graft copolymers acting as compatibilizers. In spite of these advantageous results, this procedure has not been used so far in industrial practice because of large energy consumption.

Solution blending is frequently used for preparation of polymer blends on a laboratory scale. The blend components are dissolved in a common solvent and intensively stirred. The blend is separated by precipitation or evaporation of the

solvent. The phase structure formed in the process is a function of blend composition, interaction parameters of the blend components, type of the solvent, and history of its separation. Advantages of the process are rapid mixing of the system without large energy consumption and the potential to avoid unfavorable chemical reactions. On the other hand, the method is limited by the necessity to find a common solvent for the blend components, and in particular, to remove huge amounts of organic (frequently toxic) solvent. Therefore, in industry, the method is used only for preparation of thin membranes, surface layers, and paints.

A blend with heterogeneities on the order of 10 $\mu$m can be prepared by mixing of latexes without using organic solvents or large energy consumption. Significant energy is needed only for removing water and eventually achievement of finer dispersion by melt mixing. The whole energetic balance of the process is usually better than that for melt mixing. The necessity to have all components in latex form limits the use of the process. Because this is not the case for most synthetic polymers, the application of the process in industrial practice is limited.

In partial block or graft copolymerization, homopolymers are the primary product. But, an amount of a copolymer sufficient for achieving good adhesion between immiscible phases is formed (59). In most cases, materials with better properties are prepared by this procedure than those formed by pure melt mixing of the corresponding homopolymers. The disadvantage of this process is the complicated and expensive startup of the production in comparison with other methods, eg, melt mixing.

Another procedure for synthesis of polymer blends is by formation of interpenetrating polymer networks. A network of one polymer is swollen with the other monomer or prepolymer; after that, the monomer or prepolymer is crosslinked (63). In contrast to the preceding methods used for thermoplastics and uncrosslinked elastomers, blends of reactoplastics are prepared by this method.

### Phase Structure Development in Molten State.

*Starting Period of Melt Mixing.* Most polymer blends are prepared by melt mixing and processed in the molten state. Therefore, the phase structure of a blend is formed during melt flow and is petrified by solidification. Formation of the phase structure at the initial stage of the mixing was intensively studied by Macosko's group (64–68). It was found that sheets of minor phase are formed after the start of mixing. Quite rapidly, holes are formed in these sheets that coalesce. Further, the sheets transform to fibers or co-continuous structures, which can pass (depending on blend composition and properties of the components) to a dispersed structure (see Figs. 4**a**–4**e**). If the softening or melting transition temperature of the minor phase is lower than that of the major phase, switching of phase continuity occurs at this stage of mixing (67). It was found that the reduction of characteristic size of phase domains from millimeters (characteristic size of polymer pellets) to micrometers is rapid. This reduction has been achieved during the first 2 min in batch mixers and in the first mixing zones in extruders.

*Type of Phase Structure.* For application of polymer blends, type and fineness of their phase structure are important. In blends of immiscible polymers 1 and 2 with low content of 2, particles of component 2 are dispersed in the matrix of component 1. With rising fraction of 2, partially continuous structure of 2 appears. With further increase in the amount of 2, fully co-continuous structure is formed (see Fig. 5). After that, phase inversion occurs, where 2 forms the matrix and 1

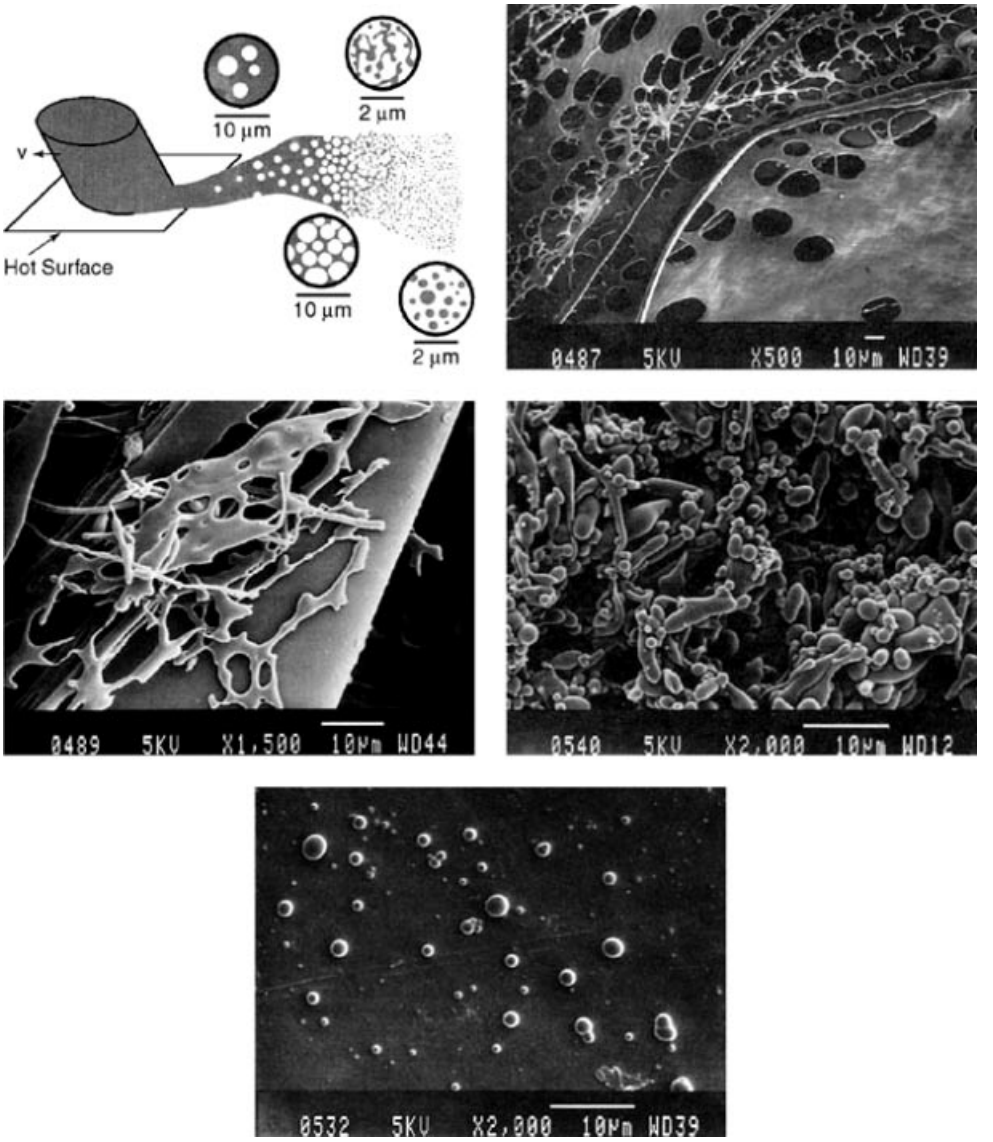


**Fig. 4.** (**a**) Scheme of initial morphology development. (**b**) Holes and lace structure observed in ribbons at 1.0 min mixing. (**c**) Broken lace structure and small spherical particles at 1.0 min mixing. (**d**) Morphology of the dispersed phase particles at 1.5 min mixing. (**e**) Morphology of the dispersed phase particles at 7 min. mixing. Reproduced with permission from Reference 64.

the dispersed phase (69,70). Dependencies of continuity indexes or percentages of continuity (the continuous fraction of a component, determined as a fraction of the component that can be dissolved with a selective solvent) on volume fraction of component 2 are schematically shown on Figure 15. In contrast to low molecular weight emulsions, where phase inversion occurs in one point or in a very narrow

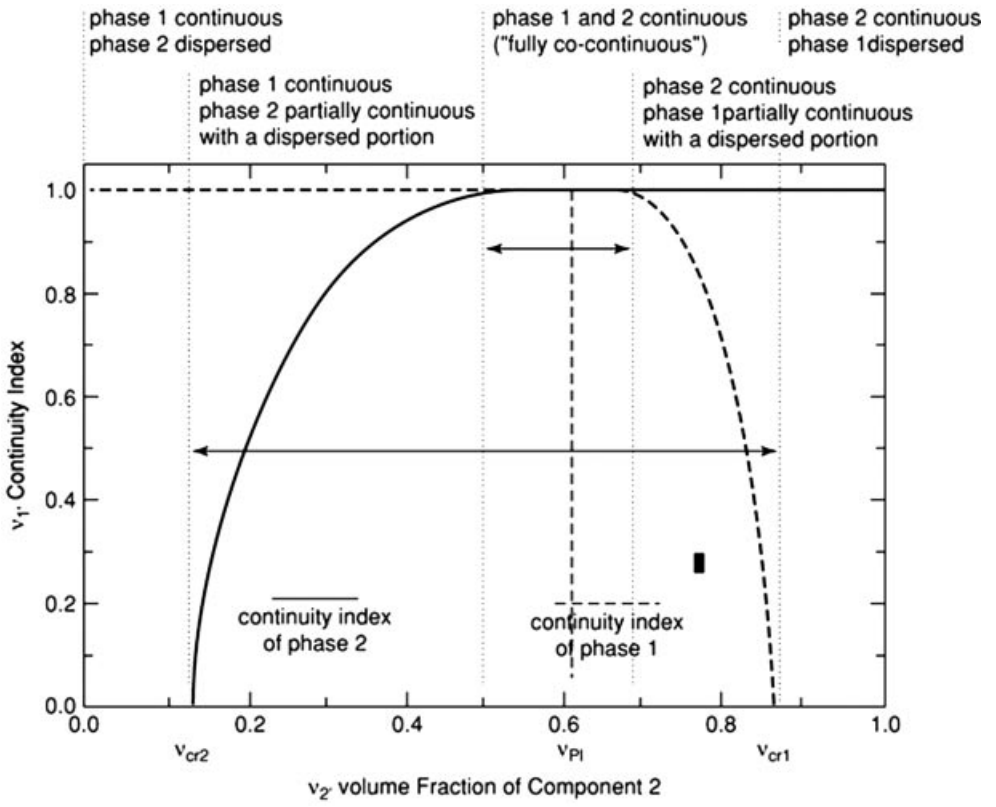


**Fig. 5.** Composition range of co-continuous structure. Full line continuity index of phase 2, broken line continuity index of phase 1. $v_{cr1}$, $v_{cr2}$, $v_{f1}$ a $v_{f2}$ are volume fractions of phase 1 or 2 at which partial or full co-continuity of the related phase start. $v_{PI}$ designate phase inversion composition. Reproduced with permission from Reference 69.

interval of composition, co-continuous range for polymer blends is frequently quite wide. Phase inversion points calculated as the center of the interval with full co-continuity of both the components and of the interval between critical volume fractions, $v_{cr1}$ and $v_{cr2}$ for starting continuity of components 1 and 2, need not be the same. The interval of volume fractions of the components in which the blend structure is co-continuous depends on rheological properties of the components, interfacial tension, and mixing conditions. There have been several attempts to formulate a rule for prediction of the phase inversion point from the knowledge of viscosity of the components (69,71–74). They qualitatively describe the experimentally verified tendency of a less viscous component to be continuous down to low volume fractions. However, all fail in quantitative evaluation of a substantial portion of experimental data (69). The proposed rules for prediction of the phase inversion from the knowledge of elastic properties of the components (75–77) contain unknown parameters or have limited validity.

Utracki and Lyngaae-Jørgensen (78) proposed a theory based on the assumption that the critical volume fractions relate to the percolation thresholds of droplets, and phase inversion appears at the composition at which the blend

with dispersed component 1 and matrix 2 has the same viscosity as the blend with dispersed component 2 and matrix 1. The theory qualitatively describes dependencies of the continuity indexes on the blend composition found experimentally. However, for some blends, $v_{cr}$ does not relate to the percolation threshold for spheres, and the predicted point of phase inversion does not agree with the experimental one for a number of systems.

A model for formation of fully co-continuous morphology based on material properties and processing conditions was proposed (79). It is based on the assumption that full co-continuity is achieved when randomly oriented cylindrical particles, formed by deformation of droplets of a minor component, are closely packed. For the volume fraction of a minor component, $v_{dl}$, at which co-continuous structure is formed, the following equation was derived

$$\frac{1}{v_{dl}} = 1.38 + 0.0213\left(\eta_m \dot{\gamma} \frac{R_0}{\sigma}\right)^{4.2} \tag{10}$$

where $\eta_m$ is viscosity of the matrix, $\dot{\gamma}$ is the shear rate, $\sigma$ is the interfacial tension, and $R_0$ is the radius of equivalent sphere related to a droplet of the minor phase. The model qualitatively describes the fact found experimentally that the width of the co-continuity interval increases with decreasing interfacial tension. Unfortunately, the model cannot be used in a predictive manner because $R_0$ has to be determined afterwards.

Recent studies (80,81) showed that at long mixing in batch mixers, transition from co-continuous to dispersed morphology appears. The mixing time, at which the transition was determined, is about one order of magnitude longer than the time necessary for reduction of the characteristic size of phase domains from millimeters to micrometers. At present, it is not clear whether co-continuous structure is only transient, or in some cases, steady (relating to certain steady mixing conditions) morphology. Elucidation of this problem is complicated by the fact that transitions between co-continuous and dispersed structures frequently occur after a long time of mixing, where it is very difficult to avoid strong degradation of the blend components.

In addition to co-continuous morphology, droplet-within-droplet (composite droplets, subinclusion, salami-like) morphologies are sometimes formed in blends with a higher content of minor component (see Fig. 6) (70,82). In some systems, ribbon like or stratified morphology was detected instead of classic co-continuous one (75). Rules for formation of individual types of morphology have not been formulated so far.

Prediction of the type of morphology in polymer blends containing three and more components is a more difficult task than for binary blends. Generally, properties of the components, interfacial tensions between them, and mixing conditions should be considered. A quite successful predictive scheme was proposed for blends with matrix component 2 and two minor dispersed components 1 and 3. It was proposed (70,83) that component 3 encapsulates the component 1 if the spreading coefficient $\lambda_{31}$ is positive. $\lambda_{31}$ is defined as

$$\lambda_{31} = \sigma_{12} - \sigma_{32} - \sigma_{13} \tag{11}$$

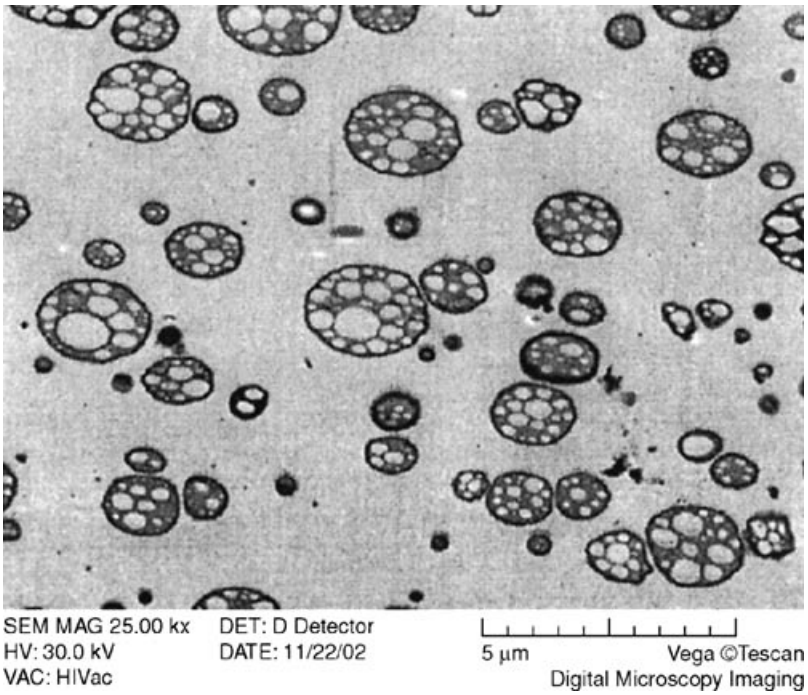


**Fig. 6.** Micrograph of droplet-within-droplet (composite droplets, subinclusion, salami-like) morphology.

where $\sigma_{12}$, $\sigma_{32}$, and $\sigma_{13}$ are the interfacial tensions for each component pair. If spreading coefficient $\lambda_{13}$ is positive, the component 1 encapsulates component 3. For both $\lambda_{31}$ and $\lambda_{13}$ negative, separated droplets of 1 and 3 are formed. The concept of spreading coefficients was extended taking into account the overall interface Gibbs free energy by including interfacial area of each component (84). Predictions of these schemes agree with a substantial number of experimental results (70,83–86), but the effect of rheological properties of the components on the type of phase structure was reported in some papers (87–89). The results of Reference 89 were plausibly explained if effective interfacial tensions, relating to flow, considering elasticity of the components were used in the predictive schemes. No rule for prediction of the continuity degree of the components is available for ternary blends.

### Binary Polymer Blends.

*Size of Dispersed Droplets in Flow.* The effects of the properties of blend components and mixing conditions on fineness of the phase structure are well understood qualitatively for binary polymer blends with dispersed structure. It is broadly accepted that the size of dispersed droplets in flowing blends is controlled by the competition between the droplet breakup and coalescence (70,90–94). On the other hand, the droplet breakup and coalescence in blends with viscoelastic components are complex events described only approximately. Moreover, the flow field in mixing devices is also complex, which further complicates correct description of the phase structure development (70,92–94).

Deformation of a droplet in a flow field is controlled by the competition of the deforming stress, $\tau$, setting on the droplet by external flow field and the shape conserving interfacial stress, $\sigma/R$, where $R$ is the droplet radius (70,90–96). For characterization of the deformation, the dimensionless capillary number, $Ca$, defined as $Ca = \tau R/\sigma$, is used. Above a critical value, $Ca_c$, the external stress overrules the interfacial stress, the droplet is stretched and finally breaks into fragments. For Newtonian droplets in a Newtonian matrix, $Ca_c$ is a function of the ratio, $p = \eta_d/\eta_m$, of the viscosities of the dispersed phase and matrix. For blends with viscoelastic components, $Ca_c$ is also a function of their elasticity parameters. A minimum $Ca_c$ was found for $\eta_d/\eta_m$ between 0.1 and 1 for shear and extensional flows. At shear flow, $Ca_c$ gradually increases with decreasing $p$ for $p < 0.1$. For $p > 1$, $Ca_c$ steeply increases with increasing $p$ and goes to infinity for $p \approx 3$–4. At extensional flow, the minimum is flat and an increase in $Ca_c$ for high and low $p$ is weak. For flow in mixing devices, the dependence of $Ca_c$ on $p$ lies between those for shear and extensional flow (94). Two main breakup mechanisms were recognized: stepwise, ie, a repeated droplet breakup into two fragments, and transient, where the droplet is stretched into a long fiber that bursts into a chain of small droplets (70,90,92–94,97). It seems that the stepwise mechanism operates for $Ca$ only slightly higher than $Ca_c$ and the transient one for $Ca \gg Ca_c$. Other breakup mechanisms such as tip streaming (or erosion) of small droplets from the surface of deformed droplets and breakup into two main and several satellite droplets were detected (70,94–96). So far, the role of individual breakup mechanisms in complex flow fields generated in mixing devices has not been fully understood, and it is the object of intensive investigation.

Flow-induced coalescence is caused by droplet collisions due to the difference in their velocities (91–94,98–100) (see Fig. 7). The coalescence is usually described in "ballistic approximation," ie, the number of fusions of droplets in a time period is expressed as a product of the number of collisions of noninteracting

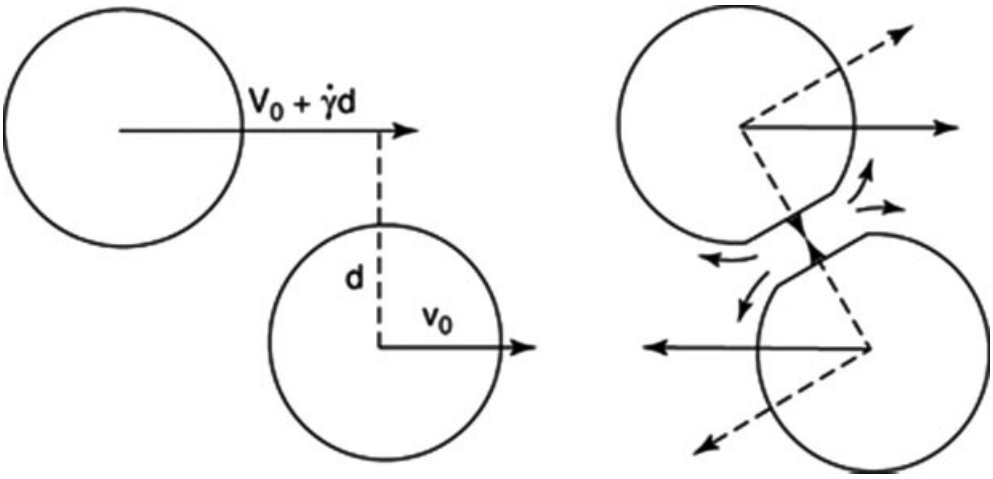


**Fig. 7.** Shear flow induced coalescence of droplets with the same coordinate in neutral direction. Forces causing droplet approach and rotation in coordinate system moving with the center of inertia are indicating.

droplets and probability, $P_c$, that the collision will be followed by droplet fusion (91,92,94,100,101). A more or less intensive flattening of the droplets appears during their collision in dependence on properties of the blend components and flow field (100,102). Most calculations of $P_c$ were focused on the case where droplets keep spherical shape during coalescence (102,103) or where the radius of flattened area is substantially larger than interdroplet distance (91,92,100). Unfortunately, the dependences of $P_c$ on system parameters are quite different in these cases. In the former case, $P_c$ is a decreasing function of $p$ and the ratio of radii of large and small droplets and is independent of the average droplet size and deformation rate. On the other hand, in the latter case, $P_c$ is independent of the ratio of droplet radii and depends on average $R$ and the deformation rate. Therefore, inadequate application of any of these extreme cases can lead to a serious misinterpretation of experimental results. Recent calculations (104,105) have shown that for deformable droplets, $P_c$ is given by the value for the spherical particles in the region of small $R$ and steeply decreases at a certain $R$ where a substantial flattening appears (for the shape of $P_c$, see Fig. 8). It should be mentioned that the so far developed theories describe dilute systems (simultaneous collisions of three and more droplets are not considered) of Newtonian droplets in a Newtonian matrix.

Generally, the distribution of droplet sizes in flow can be obtained as a solution of the generalized Smoluchowski (balance population) equation describing the competition between the droplet breakup and coalescence. Various approximate approaches to the solution of the equation with various expressions for breakup and coalescence frequencies have been used in the literature (101,105–115). For rather long mixing in batch mixers, achievement of a steady state in the droplet size distribution is assumed. For mixing in extruders, development of the droplet

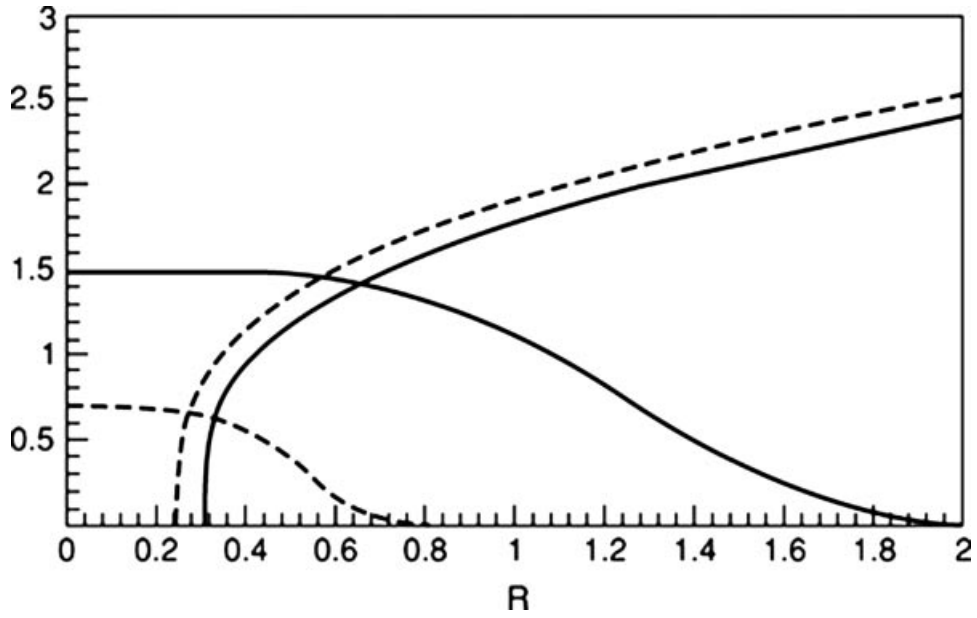


**Fig. 8.** Scheme of graphic solution of equation 12. Full and broken lines relate to blends with and without a compatibilizer. $Y$-axis shows $F(R)$ and $(4/\pi)\dot{\gamma}vP_c(R)$ in arbitrary units.

size distribution during throughput in individual zones of the extruders should be studied. A simplified model, where a system of droplets is still monodisperse and breakup leads to a decrease and coalescence to an increase in droplet size, can be helpful in understanding the dependence of average droplet size on parameters of a system (116). The steady droplet radius for this model in shear flow can be calculated from the equation (116)

$$\left(\frac{\mathrm{d}n}{\mathrm{d}t}\right)_{\mathrm{B}} = \left(\frac{\mathrm{d}n}{\mathrm{d}t}\right)_{\mathrm{C}} \Rightarrow F(R) = \left(\frac{4}{\pi}\right)\dot{\gamma} v P_{\mathrm{c}}(R) \tag{12}$$

where $(\mathrm{d}n/\mathrm{d}t)_{\mathrm{B}}$ and $(\mathrm{d}n/\mathrm{d}t)_{\mathrm{C}}$ are changes in the droplet number in a time unit due to their breakup and coalescence, respectively, and the breakup frequency $F(R) = 0$ for $R < R_{\mathrm{c}} = \sigma Ca_{\mathrm{c}}/(\eta_{\mathrm{m}}\dot{\gamma})$. The dependence of $F$ on $R$ for $R > R_{\mathrm{c}}$ has not been well established, and very different expressions have been used in literature (116). It seems, based on recent results, that $F$ increases with $R$ slower than linearly (96, 117). This assumption is in agreement with experiments showing a steeper than linear increase in $R$ with increasing $v$ in a certain blend under constant mixing conditions (70,90,93,94,116). In spite of the approximations used in calculation of $P_{\mathrm{c}}$, the shape of the dependence $P_{\mathrm{c}}$ on $R$ is always similar to that in Figure 8. It follows from graphic solution of equation 12, shown in Figure 8, that for $R_{\mathrm{c}}$ smaller than $R$, at which $P_{\mathrm{c}}$ falls to very low value, steady state can be achieved during reasonable time. In the opposite case, regions of $R$ exist where only coalescence or practically only breakup occurs.

Under constant mixing conditions, an increase in average droplet radius with increasing volume fraction of the dispersed phase has been observed (70,93,94,99,106,118). The increase is a consequence of the fact that the breakup frequency is in first approximation independent of $v$, but the frequency of coalescence is an increasing function of $v$. An increase in interfacial tension leads to an increase in $R$ (118) due to a decrease in $Ca$. The effect of viscosity ratio, $p$, can be directly studied by changing $\eta_{\mathrm{d}}$ while keeping $\eta_{\mathrm{m}}$ constant. For a system containing a low $v$, the effect of $p$ on droplet breakup is decisive and the dependence of $R$ on $p$ for stepwise breakup is controlled by the dependence of $Ca_{\mathrm{c}}$ versus $p$. For a transient breakup mechanism, the situation is different and an increase in $p$ can lead to smaller $R$ also for $p > 1$ (91,92,112). Generally, $P_{\mathrm{c}}$ decreases with increasing $p$. Therefore, a lower $R$ at $v \to 0$ and a steeper increase in $R$ with $v$ should appear for lower $p$ if the stepwise breakup mechanism is decisive. This type of dependency was observed for polypropylene/ethylene-propylene elastomer blends mixed in the chamber of a Plasticorder (94,119). For the transient breakup mechanism, $R$ should be smaller for larger $p$ for all volume fractions of the dispersed phase. If $\eta_{\mathrm{m}}$ is changed at a constant $\eta_{\mathrm{d}}$, $p$ and $Ca$ are changed simultaneously. In most cases, an increase in $\eta_{\mathrm{m}}$ at constant $\eta_{\mathrm{d}}$ and mixing conditions leads to a decrease in the droplet size in the whole concentration range (94,119). The effect of elasticity of the components has not been fully understood so far. Available experimental results show that the deformation and breakup of droplets more elastic than the matrix are more difficult than in the related Newtonian system (70,120,121). Generally, the dependence of the droplet size on shear stress (mixing intensity) is affected by the concentration of the dispersed phase because $R_{\mathrm{c}}$ ($R$ for $v \to 0$) depends on stress (deformation rate) in a different way than $P_{\mathrm{c}}$.

While $R$ in dilute blends typically decreases with increasing stress applied during mixing (94,122–124), in concentrated systems, $R$ is a complex function of system parameters and it can be a decreasing, increasing, or nonmonotonic function of the applied stress (70,94,125,126). Only a weak dependence of $R$ on processing parameters was frequently observed (70,127–129), apparently due to a non-Newtonian character of the matrix, increase in temperature in a mixer at growing mixing rate, and increasing $P_c$ with decreasing $R$. Usually, quite fine morphology is achieved after a short time of mixing in batch mixers or in first zones of extruders (64–68,70,128–130). On the other hand, large particles of dispersed phase with high viscosity surrounded by material with fine phase structure were found in blends with low interfacial tension (94,131–133). Uniform fine morphology was achieved in these systems only after long and intensive mixing.

*Phase Structure Evolution During Annealing.* Substantial changes in the phase structure of molten blends of immiscible polymers appear at rest, and are driven by the tendency to achieve a minimum interfacial area. Deformed (elongated) droplets either retract to spheres or break up into smaller fragments. Relaxation occurs by one of several mechanisms, depending on initial deformation (the ratio of long and short semiaxes $a/b$) and the viscosity ratio (96,134,135). A droplet with the $a/b$ less than approximately 9 retracts to a single sphere. Very elongated droplets (about $a/b > 60$) break up by the capillary wave (Rayleigh) instability, ie, by the transient breakup mechanism mentioned above, into a chain of small droplets. In this case, the amplitude of the perturbation wave grows exponentially with time and the growth rate increases with interfacial tension and decreases with viscosity of both the components and fibril radius (70,91–94,96). For droplets with intermediate deformation, the breakup is dominated by end pinching (96,134,135). Co-continuous structures stay either co-continuous and show increase in the phase size with time or break up into droplet/matrix morphologies (136,137). The breakup of fibers between crossing points of the structure is controlled by the capillary wave mechanism and it can occur if the length of fibers between the crossing points is substantially larger than the fiber thickness. Therefore, the coarsening of co-continuous structures is typical of blends with compositions near 1/1 and their breakup appears for blends with asymmetric compositions. The coarsening rate increases with interfacial tension and decreases with the viscosity of blend components (137). A substantial increase in the size of dispersed particles after annealing in the molten state was found for many polymer blends with particulate morphology (138). Two main mechanisms were suggested: coalescence driven by molecular forces and Brownian motion (139), and Ostwald ripening (140,141). Analysis of these mechanisms showed that the rate of coarsening should increase for coalescence and decrease for Ostwald ripening with increasing interfacial tension (138). A clear increase in the coarsening rate with interfacial tension was found experimentally (138). Moreover, coalescing droplets were detected in some experiments (142,143). Therefore, it seems that the coalescence induced by molecular forces and Brownian motion is the main mechanism of droplet coarsening, at least for blends with moderate or high interfacial tension.

**Blends Containing a Compatibilizer.**

*The Effect of Compatibilizer on a Blend Microrheology.* The presence of a compatibilizer at the interface substantially affects the development of the phase structure of molten blends in the flow and quiescent state. The position

and width of the concentration region related to co-continuous morphology are affected by two competing mechanisms. A decrease in interfacial tension caused by a compatibilizer favors the formation and stability of co-continuous structures. On the other hand, the compatibilizer suppresses the coalescence, which is assumed to be a reason for the co-continuity formation (69). Experimentally, narrowing of the concentration region with co-continuous structure was observed for some systems (69,144,145), but no change was found in other systems (69,146,147). Fixation of co-continuous structure in a blend containing 20% of minor component by the addition of a compatibilizer was also observed (148).

The effect of a compatibilizer on fineness of the phase structure can be understood through its effects on droplet breakup and coalescence. The decrease in interfacial tension mentioned above leads to a decrease in the critical droplet radius, $R_c$, at a constant $Ca_c$. Generally, $Ca_c$ of a compatibilized blend differs from that of the related binary blend without compatibilizer (149,150). The bulk flow convects the compatibilizer towards the ends of the droplets causing a gradient in interfacial tension along the droplet surface. The lower interfacial tension on the tips promotes tip streaming, tending to reduce $Ca_c$. On the other hand, Marangoni stresses oppose deformation. An increase in the droplet surface due to deformation leads to compatibilizer dilution and, therefore, to an increase in interfacial tension. The last two effects tend to increase $Ca_c$ (149,150). At breakup by the transient mechanism, a compatibilizer causes an increase in the breakup time due to a decrease in interfacial tension and existence of interfacial tension gradients (149–151). A decrease in interfacial tension due to the presence of a compatibilizer decreases the droplet radius, $R$, at which the probability of coalescence, $P_c$, falls to a negligible value. Two other mechanisms contributing to coalescence suppression were proposed (149,152). The first involves immobilization of the interface (suppression of liquid circulation in droplet) due to the Marangoni stress. The Marangoni stress is induced by convection of a compatibilizer out of the gap between approaching droplets, which leads to a gradient of interfacial tension (149,150). The immobilization of the interface decreases $P_c$ for small $R$. The other mechanism, repulsion of the droplets arises mainly from the compression of the compatibilizer block extending into the matrix phase (149,152). This mechanism is applied only if the dilution of a compatibilizer in the gap between droplets is not large. The effect of a compatibilizer on the breakup frequency and $P_c$ (decrease in interfacial tension and the Marangoni effect are considered) is schematically illustrated in Figure 8. Figure 8 shows that the situation when steady state is not achieved is more probable for blends with a compatibilizer. In the calculation of steady $R$, changes in interfacial tension induced by changing interfacial area in droplet breakup and coalescence should be considered (153). The above effect can be quantified if the distribution of a copolymer between the interface and bulk phases, relationship between copolymer concentration at the interface and interfacial tension, and the rate of copolymer migration along the interface and between the interface and bulk phases are known.

*Effect of the Compatibilizer Architecture.* Compatibilization efficiency of various copolymers follows from their thermodynamic and microrheological effects. It has been generally accepted that the total molecular weight of the copolymer, molecular weight of its blocks and their number are the main structural compatibilizer characteristics affecting the phase structure of the final blend.

Contradictory results have been published on the effect of block copolymers with different numbers of blocks. In some papers, diblock copolymers have been found more efficient compatibilizers than triblock copolymers (51,154,155), whereas in several other studies, the opposite results have been obtained (156–158). Still others state that there is no difference between diblocks and triblocks (159). Some more recent articles show the compatibilizing efficiency of multiblock (tetrablock, pentablock, heptablock) copolymers (160–162), which seems to be supported also by some theoretical studies (163,164).

It has been believed that proper molecular weight of the copolymer blocks should be close to that of the relevant homopolymer. However, some results show that copolymers with differing lengths can be efficient compatibilizers. A complex situation also occurs when the copolymer blocks are not chemically identical with homopolymer chains, but only similar, and thus they exhibit limited miscibility. The complexity of these issues have been shown in a number of studies.

Thus Xu and Lin (154) successfully compatibilized a high molecular weight blend of *i*PS and *i*PP with a *i*PS-*i*PP diblock copolymer, where the molecular weight of both blocks amounted to 150,000. Feng (165) has shown that for PS/polyolefin blends, even PE-*g*-PS graft copolymers can be suitable compatibilizers.

Cavanaugh and co-workers (166) have studied the compatibilization efficiency of various styrene-butadiene copolymers in polystyrene (PS, $M_w$ = 202,000)/polybutadiene (PB, $M_w$ = 320,000) blends. The most effective compatibilizer proved to be a long, asymmetric diblock ($M_w$ = 182,000; PS content 30%), which could entangle in both homopolymer phases. Short diblock copolymers and most of the random copolymers were inadequate as interfacial agents. Moderate improvement in impact strength was observed for a S-B multiblock.

The effects of the block length and block number in linear S-B block copolymers on compatibilization efficiency in low molecular weight PS/PB blends were studied also by Horák and co-workers (167). For this detailed stucture study, PS ($M_w$ = 40,000), PB ($M_w$ = 60,000), and di-, tri-, and pentablock S-B copolymers, having $M_w$ of the PS block either 10,000 or 40,000, were prepared. Besides standard slow cooling, also quenched samples, having the structure close to that of the molten state, were prepared. It shows that in quenched samples, all block copolymers, with an exception of large 40S–60B–40S, are molecularly dispersed (probably at the PS/PB interface). Escape of the S-B copolymers from the interface is observed for the copolymers having short PS blocks, while the copolymers with long PS blocks remain a part of the PS/PB interfacial layer, and this phenomenon manifests itself by the formation of a finer morphology and better stress-transfer properties than in blends containing S-B copolymers with short PS blocks.

Segregation of a poly(2-vinylpyrrolidone-*block*-styrene-$d_8$-*block*-2-vinylpyrrolidone) (PVP-dPS-PVP) triblock and dPS-PVP diblock copolymers between the PS and PVP homopolymers was studied by Dai and co-workers (169). Both the block copolymers show an increase in the interfacial excess beyond the saturation plateau, due to condensation of copolymer micelles adjacent to the PS/PVP interface in the PS phase (Fig. 9). A significantly lower critical micelle condensation (CMC) was determined for the triblock copolymer when compared with the diblock. While the condensation of the diblock copolymer micelles at the PS/PVP surface occurs above the CMC, no such preferential segregation is observed for the triblock copolymer.

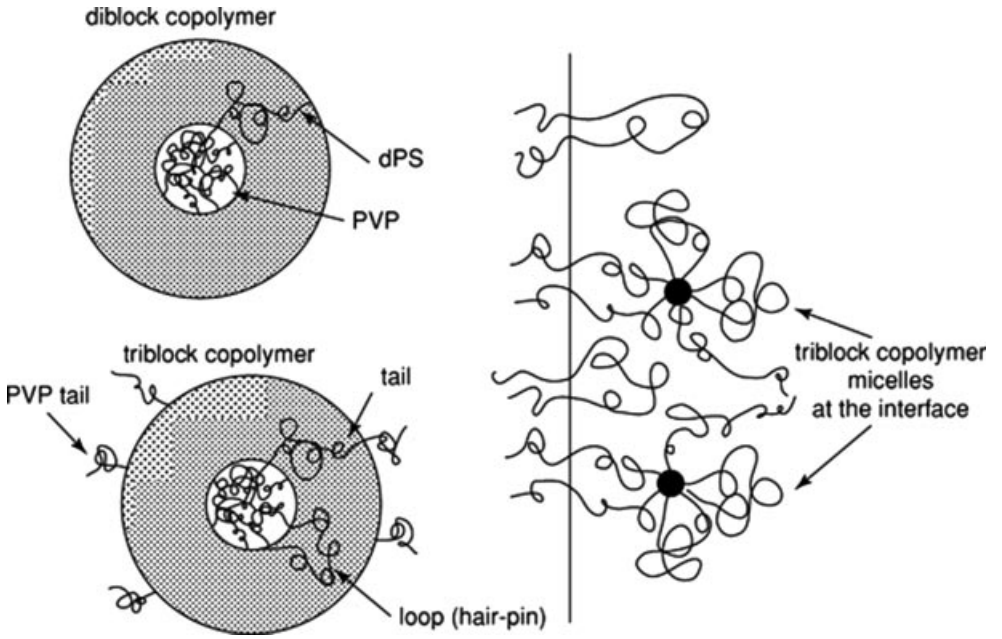


**Fig. 9.** Condensation of PVP-dPS-PVP triblock copolymer micelles adjacent to the PS/PVP interface in the PS phase. Schematics of (left) the isolated micelle structure for diblock and triblock copolymers and (right) triblock copolymer micelles adsorbed onto an interfacial brush of triblock copolymers.

The compatibilization process becomes more complicated when one of the copolymer blocks is not completely miscible with the corresponding blend component, ie, interaction parameter $\chi > 0$. This problem has been studied in polystyrene (PS)/polyolefin (PO) blends compatibilized with various block copolymers, consisting of styrene and aliphatic hydrocarbon sequences different from the used polyolefin (161,162,168,170–173). It was found that in these blends, the most important factor controlling localization of the block copolymers at the PS/PO interface is the length of the styrene block in the block copolymers. Copolymers having the styrene blocks long enough to form entanglements with the styrene homopolymer in the blend, are entrapped in the final compatibilized blends in this phase. Hence, their transport to the PS/PO interface is difficult and their compatibilization efficiency is low. Critical molecular weight for the formation of the entanglements of PS chains, $M*$, cca 18,000 was determined (174,175). Surprisingly, in these blends, block copolymers with "long" styrene blocks are less efficient compatibilizers than those with "short" blocks.

Also the interfacial layer between the homopolymers differs in A/B + A-*block*-B' blends from that in A/B + A-*block*-B blends. In blends compatibilized with block copolymers having the corresponding blocks miscible with the blend components, they are supposed to be molecularly dispersed to a high degree at the A/B interface (Figs. 9, 3). In A/B/A-*block*-B′ blends, block copolymers with "short" A blocks are localized at the A/B interface as well, but they do not lose their ordered supermolecular structure (Fig. 10). Block copolymers having "long" A blocks are

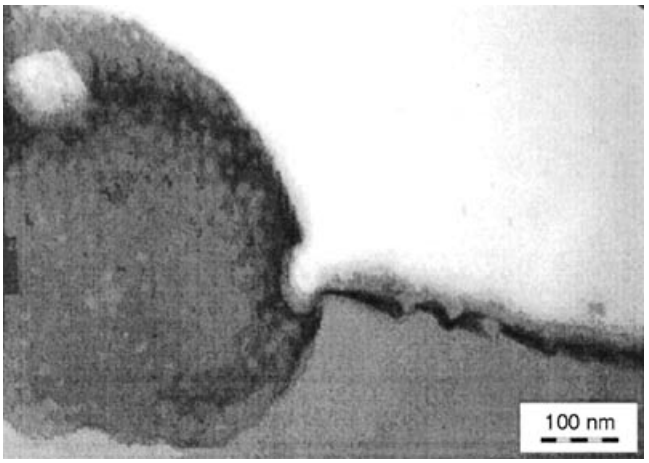


**Fig. 10.** TEM micrographs of the interface in PS/PP (4/1) blend with addition of 10S-60B-10S block copolymer.

entrapped in the A homopolymer in the form of micelles or small particles, swollen by homopolymer chains (Fig. 11**a**). Additional annealing of these blends leads to pronounced migration of the entrapped copolymers to the A/B interface (Fig. 11**b**) and improvement of mechanical properties. On the other hand, coalescence and worsening of the A/B interface coverage were observed in annealed blends on addition of copolymers having "short" styrene blocks (168). In general, morphology of the A/B/A-*block*-B′ blends depends on the conditions of blend mixing and processing, and cannot be predicted using only the rules of equilibrium thermodynamics. This dependence on the processing conditions is more pronounced in blends with an excess of the A phase, ie, of the homopolymer that is fully miscible with one block of the block copolymer used (168).

Different behavior of block copolymers having blocks miscible with the corresponding homopolymers and those where one block differs chemically from the

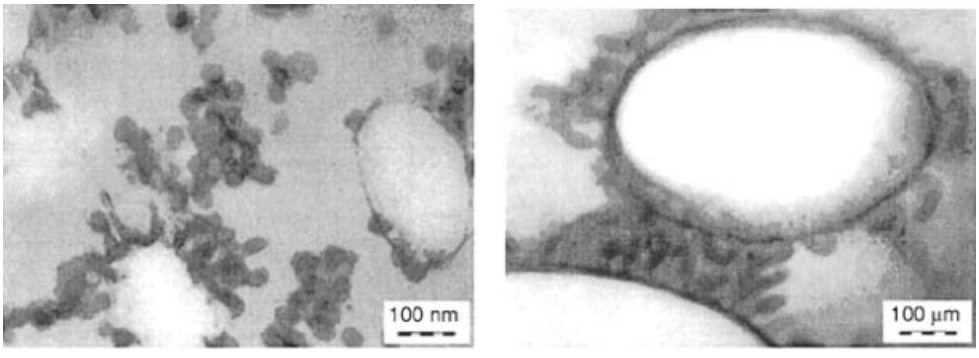


**Fig. 11.** TEM micrographs of the interface in PS/PP (4/1) blend with addition of 40S-60B-40S block copolymer: (**a**) as prepared sample; (**b**) annealed sample.

homopolymer was observed also by other authors. Barlow and Paul (176) and Appleby and coworkers (157) reported remarkable improvement of ductility and impact or tensile strength in PS/PP blends compatibilized by the commercial material Kraton G1652. This poly(styrene-*block*-ethene-*co*-butene-*block*-styrene) (S-EB-S) triblock copolymer has an $M_n$ value of one PS block approximately equal to 8,000, that is, considerably below the critical value $M*$ necessary for the entanglement formation. Tjong and Xu (177) found that the presence of this BC in PS/high density polyethylene blends leads to increased adhesion between the two phases as well as decreased particle dispersion. Cigana and co-workers (178) observed improvement of mechanical properties in PS/ethene-*co*-propene rubber blends (PS/EPR) with Kraton G1652, unlike with the S-EB-S triblock copolymer, where the molecular weight of the S block was about 24,000 (Kraton G1651).

In the PS/EPR blends, Radonjič and co-workers (179) found the S-B-S triblock copolymer with $M_n$ of the PS blocks of 7,000, to be localized at the PS/EPR interface. The compatibilization efficiency of this block copolymer was further confirmed by finer dispersion in the resulting PS/EPR/S-B-S blends, as well as by improved PS/EPR adhesion. This short triblock copolymer appears to be a good compatibilizer also in *i*PP/*a*PS blends. According to Šmit and Radonjič (180), S-B-S forms an interfacial layer between dispersed honeycomb-like PS/S-B-S particles and PP matrix and influences also crystallization in *i*PP.

Hence, the compatibilization efficiency of block and graft copolymers is influenced by many factors, such as their chemical composition with respect to the character of the corresponding blend components, the number of the blocks, their molecular weights, and consequently, the total molecular weight. Also, in blends where one block of a compatibilizer is not miscible, but only compatible with, the corresponding blend component, achievement of thermodynamic equilibrium can be difficult, as it depends on the processing conditions. However, it seems that triblock copolymers can be considered the most efficient compatibilizers for most of the blends studied.

We can conclude that despite extensive studies performed during more than three decades, no reliable rules for the prediction of the effect of molecular characteristics of block copolymers on the structure and properties of polymer blends have been formulated to date.

*Effect of Compatibilizer Concentration.* The compatibilizing efficiency of the copolymers is, besides the architecture, a function of their concentration. The effect of a compatibilizer concentration has been quantitatively characterized by the emulsification curve—the dependence of the average particle diameter of the minor dispersed phase on copolymer concentration (70). The particle diameter decreases with increase of copolymer concentration until a constant value is obtained. For most systems, this value is achieved if the copolymer amount is 15–25% of the dispersed phase. There are systems where saturation was detected only at substantially higher concentration of a copolymer (181).

**Structure Determination of Polymer Blends.** Properties of polymer blends are closely associated with their structure on several scale levels, such as crystallinity and supermolecular structure of the blend components, and, of course, morphology of the final blend. Thus, a series of methods that enable one to characterize these different structure parameters should be employed, including WAXS, SAXS, SANS, SEM, TEM, LS, and DSC.

Wide angle X-ray scattering (WAXS) affords information on the level of interatomic distances, ie, this method can be used for determination of crystalline modification in partially crystalline polymers, degree of crystallinity. Also, dimensions of the crystallites can be estimated from the width of the crystalline reflections (182). Small-angle X-ray scattering (SAXS) experiments lead to determination of supermolecular structure, such as ordered two-phase separation in block copolymers (183,184), long period in semicrystalline polymers (185), or micellar structure (186,187). Classic experimental techniques used in SAXS have been reviewed by Stein (188). Small-angle neutron scattering (SANS), a related and often complementary method to SAXS, is also a very useful tool for determination of supermolecular structure in polymer blends (189). Moreover, by using SANS, interactions in polymer blends can be studied if one of the blend components is deuterated in order to obtain scattering contrast (190). Recently an ultrasmall-angle neutron scattering spectrometer (USANS) was developed (191), lifting the upper resolution limit of SAXS and SANS instruments by an order of magnitude, and thus permitting an overlap with light scattering techniques.

The most suitable and comparatively rapid method used for determination of the morphology of polymer blends appears to be electron microscopy. Techniques employed in scanning electron microscopy (SEM) have been reviewed by Shaw (192). In addition to the use of SEM for determination of particle size and shape in a blend, and adhesion between the blend components (193, Fig. 12), evolution of the structure based on the processing conditions and blend homogeneity can be quickly studied (194, Figs. 13, 14). Transmission electron microscopy (TEM) is a much more time-consuming method. Polymer samples need to be stained with $OsO_4$ or $RuO_4$ in order to obtain sufficient contrast, and in addition, very thin sections are necessary (195,196). The simplest result obtained by means of TEM is, similarly to SEM, description of the blend morphology. However, there is a wider scale of possibilities, such as localization of a block copolymer used as a compatibilizer in blends of immiscible polymers (197). Chi-An Dai and co-workers (198) published a study of the morphology development of poly(2-vinyl pyrrolidone)-*block*-(deuterated polystyrene)-*block*-poly(2-vinyl pyrrolidone

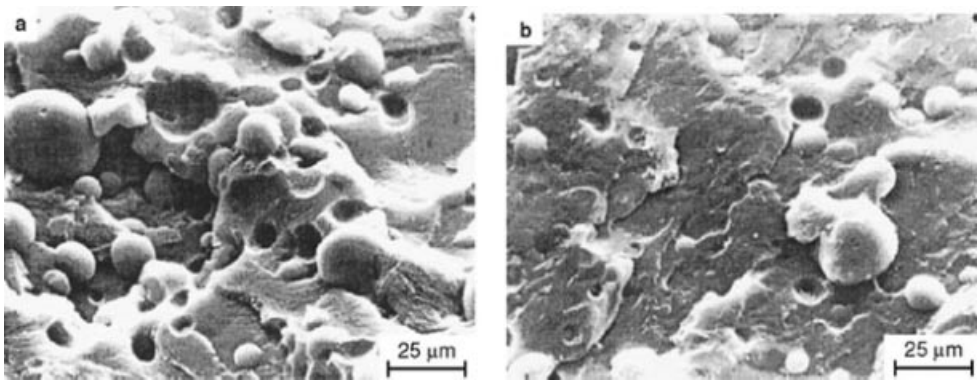


**Fig. 12.** Scanning electron micrographs of cryofractured surfaces of HDPE/HIPS (80/20) blend with H77 copolymer concentration of: (**a**) 0 wt%, (**b**) 5 wt%.

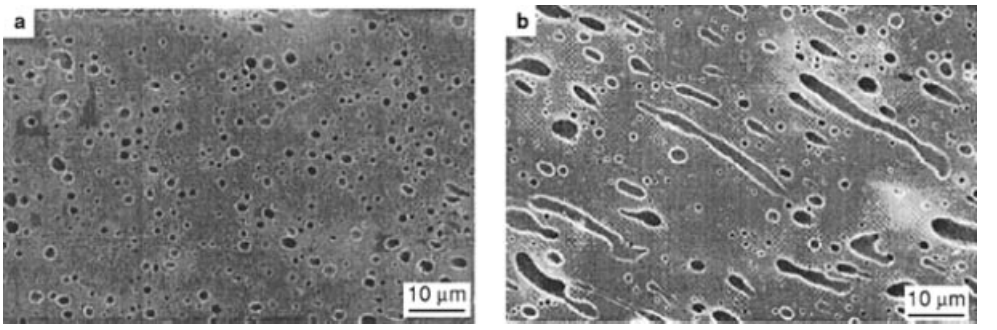


**Fig. 13.** Phase structure of PP/PS/SBS (71/24/5) blends mixed in microextruder at 250°C for 2 min: (**a**) small particles; (**b**) large particles.

(PVP-*block*-dPS-*block*-PVP) triblock copolymer at the PS/PVP interface, observed by TEM (Fig. 15).

Light scattering can be used for determination of the blend morphology, not only in the solid, but also in the molten state (199,200). This method was successfully used in detection of phase transitions in polymer blends, and in determination of changes in droplet size in immiscible polymer blends due to breakup and/or coalescence. In comparison with microscopic methods, scattering methods can easily examine larger blend volume, and therefore, give more reliable average values of morphological parameters. On the other hand, microscopic methods provide more straightforward and complex information (201).

Differential scanning calorimetry (DSC) is used especially for discrimination between miscible and immiscible polymer blends (202). One $T_g$ depending on blend composition indicates a miscible system, two $T_g$ coinciding with related $T_g$ of the components indicate an immiscible blend, and two $T_g$ shifted to the direction of their average is typical of partially miscible systems.

As polymer blends are very complex systems, a combination of different methods for complete description of their structure is of great importance. Several examples of typical combinations are described below.

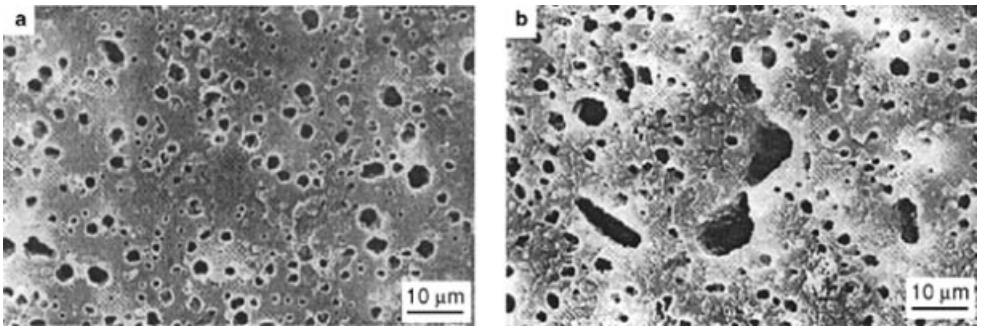


**Fig. 14.** Phase structure of PP/PS/SBS (71/24/5) blends mixed in microextruder at 250°C for 20 min: (**a**) smaller particles; (**b**) larger particles.

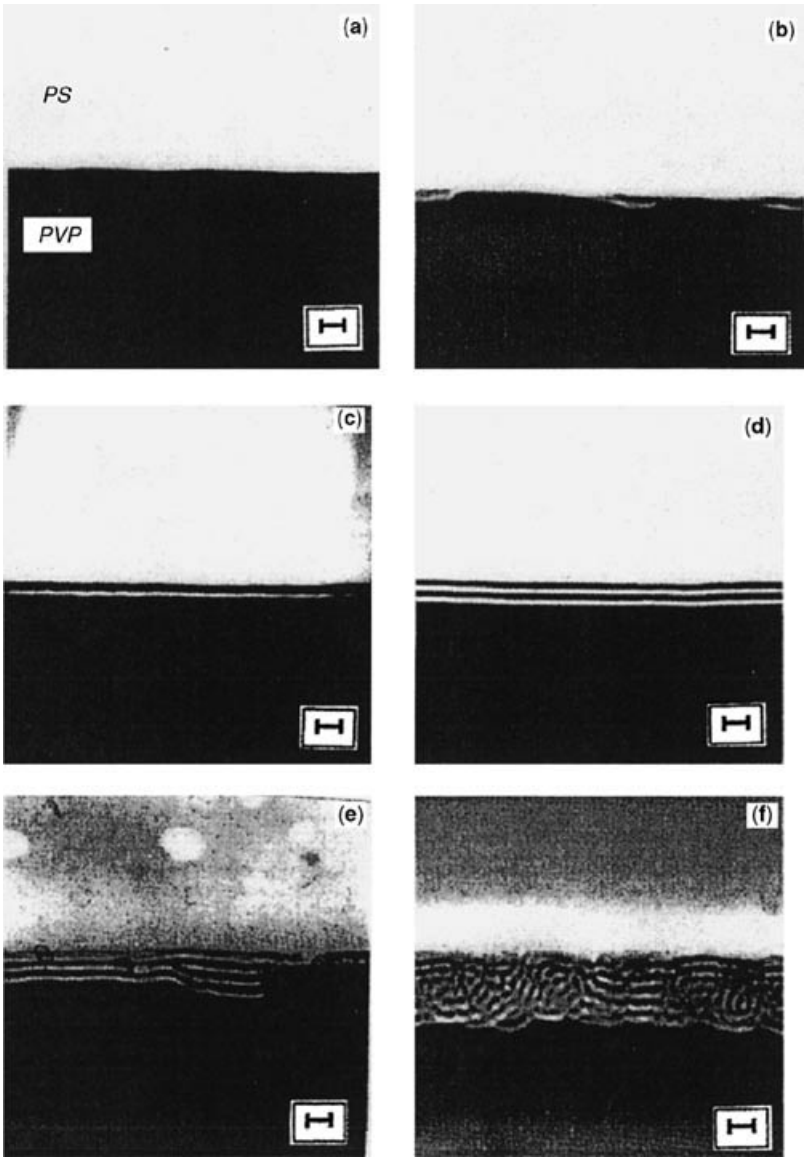


**Fig. 15.** TEM micrographs of the morphology of the PVP-dPS-PVP triblock copolymer microstructure near the interface for (**a**) area chain density, $\Sigma = 0.09$, (**b**) $\Sigma = 0.17$, (**c**) $\Sigma = 0.22$, (**d**) $\Sigma = 0.4$, (**e**) $\Sigma = 0.6$, (**f**) $\Sigma = 1.0$ chains/nm$^2$. Note that disordered lamellae are found for $\Sigma > 0.6$ chains/nm$^2$. The bar scale denotes 100 nm.

Combination of WAXS and SAXS is a very efficient way of detailed description of crystallization in blends of semicrystalline polymers. Baldrian and co-workers (203,204) has studied isothermal melt crystallization of blends of low molecular weight poly(ethylene oxide) (PEO) and poly(methyl methacrylate) (PMMA) using time resolved SAXS/WAXS measurements on the ELETTRA synchrotron (205). He has reported the formation of unstable PEO lamellae of nonintegrally folded

chains at the very beginning of crystallization and subsequent transformation of these lamellae into stable PEO crystals with one-folded or extended chains. Amorphous PMMA plays a decisive role in structure development. A similar study was performed by Campoy and co-workers (205) with polyamide (PA6) and the liquid-crystalline copolyester Vectra using calorimetric data and X-ray diffraction.

Structure development in blends of polyaniline doped with camphor sulfonic acid (PANI-HCSA) and PA was studied by Hopkins and co-workers (206) using SAXS and SANS. At 3 vol% PANI loading concentration, salt domains with characteristic length of 22 nm are expected to be present in the blend with PA12. This differs from the blend of PA6 where a fractal geometry was found. For higher salt concentrations, no simple structural model was found.

Wignal and co-workers (207) investigated phase separation of linear (high density) and short-chain branched (linear low density) polyethylenes (HDPE/LLDPE) by of combination of SAXS, SANS, DSC, and TEM. According to SANS, this blend is homogeneous in the melt when the ethyl branch content in LLDPE is low, but due to the structural and melting point differences between HDPE and LLDPE, the components may phase-separate in the solid state.

Block copolymers, usually used as compatibilizers in additive compatibilization, are very often organized in an ordered supermolecular structure, which manifests itself by an interference maximum in the region of SAXS (183,184). The compatibilization efficiency of a block copolymer is associated with its interaction with the blend components, and consequently, with the changes of its supermolecular structure. Hence it is convenient to begin the study of its structure in compatibilized blends using SAXS. Additionally, SAXS gives information on a comparatively large sample volume, even if the information concerns the reciprocal space. Microscopic methods show the real structure, but of a very small part of the sample, which can be inhomogeneous. Thus, combination of scattering and microscopic methods appears to be a very useful for investigation of the compatibilization process. Moreover, TEM and SEM experiments are relatively time consuming, while measurement of one SAXS curve takes several minutes. Thus, it is possible to check samples obtained under preparation conditions, when the steady state is achieved by comparison of SAX curves. Then, several selected samples can be studied by electron microscopic methods (168). Kinning shows in his study (208) a very instructive comparison of different orderings of a styrene-butadiene block copolymer in a styrene homopolymer, obtained by TEM together with corresponding SAXS curves (Figs. 16, 17)

## Physical Properties of Polymer Blends

Preparation of heterogeneous polymer blends ranks among the effective ways of upgrading polymers and preparing new cost-effective materials. Tensile modulus, $E_b$, or shear modulus, $G_b$, tensile yield strength, $\sigma_{yb}$, tensile strength (stress at break), $\sigma_{ub}$, fracture resistance, permeability, $P_b$, to gases and vapors, etc. are viewed as very important physical properties that simultaneously predetermine possible applications of the blends of industrially useful polymers. Phase structure (morphology), which depends on blend composition, relative viscosities of components, interfacial energy, mixing machine and adopted conditions of the mixing

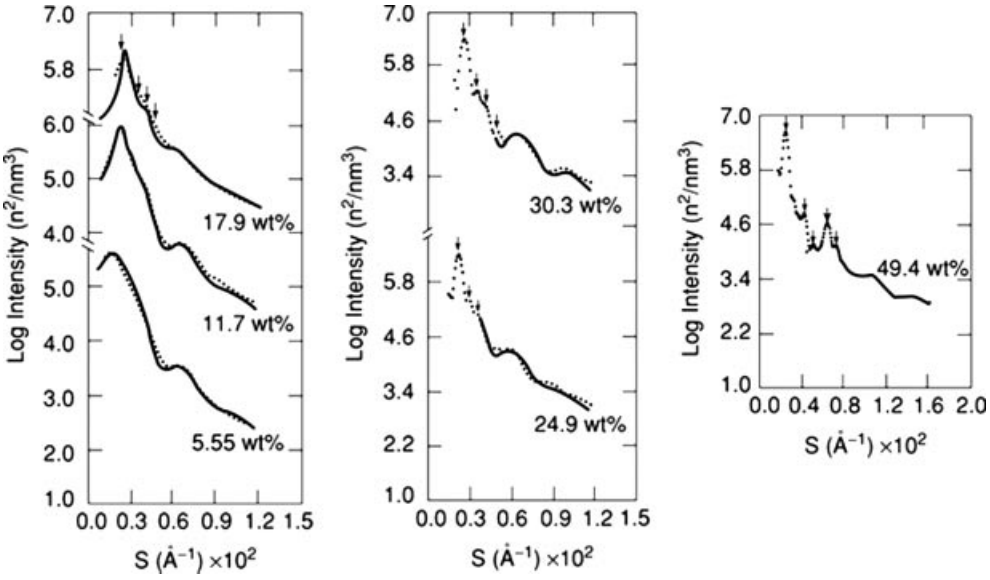


**Fig. 16.** SAXS curves of blends consisting of copolymer SB 20/20 in 3900 PS homopolymer at various copolymer concentrations.

process, annealing, reprocessing, etc., is essential for the properties of heterogeneous melt-mixed blends consisting of immiscible or partly miscible polymers (209,210). As the phase structure of a blend formed in a mixing machine does not correspond to a state with the lowest Gibbs free energy, the phase structure

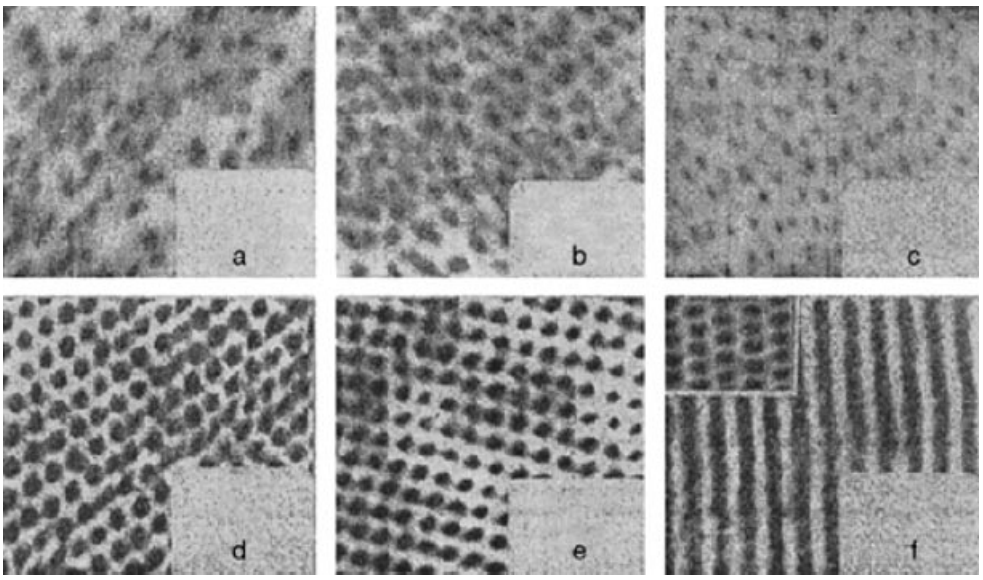


**Fig. 17.** Transmission electron micrographs of blends containing copolymer SB 20/20 in 3900 PS homopolymer. Copolymer concentrations are (**a**) 5.55 wt%, (**b**) 11.7 wt.%, (**c**) 17.9 wt%, (**d**) 24.9 wt%, (**e**) 30.3 wt%, and (**f**) 49.4 wt%. The bar scale denotes 100 nm.

coarsening begins to take place immediately after completion of the mixing process and is stopped only by freezing-in the melt. The coarsening process is reinitiated whenever blends are heated to processing temperatures in the course of following operations, such as injection or compression molding, reprocessing, and quiescent annealing. In practice, the coarsening is undesirable phenomenon because it usually accounts for deterioration of physical (mechanical) properties of annealed or reprocessed blends.

Heterogeneous blends of immiscible or partially miscible polymers are isotropic heterogeneous materials with three-dimensional spatial continuity of one or more components (69,211). In binary blends, the co-continuity (duality) of constituents occurs in the central composition interval delimited by the critical fractions, $v_{1cr}$ and $v_{2cr}$, of the components (69,78,212,213). From the viewpoint of mechanical properties, blends can be divided into two basic categories: (1) at $v_1 < v_{1cr}$ or $v_2 < v_{2cr}$, the minority component is dispersed as spherical particles in the continuous majority component (matrix); (2) at $v_1 > v_{1cr}$ and $v_2 > v_{2cr}$, both components become partially continuous. As soon as the volume fraction of a component exceeds $v_{cr}$, continuous entities are formed in the mixed blend, but a spectrum of particles still coexists. With increasing volume fraction, the degree of continuity (continuity index) of the component increases, so that in a narrower interval delimited by the volume fractions $v_{1dl} > v_{1cr}$ and $v_{2dl} > v_{2cr}$, both components are fully co-continuous (213–215). The coarsening process manifests itself by narrowing the interval of the phase duality and/or by an increase in the particle size of the minority component. Physical properties of solid heterogeneous blends primarily depend on respective properties of the components, frozen-in phase structure, and interfacial adhesion. Typical dependencies of physical properties on the blend composition are schematically visualized in Figure 18.

**Predictive Formats for Selected Physical Properties of Polymer Blends.** Tailoring of heterogeneous polymer blends with balanced physical properties for specific applications is a frequent task of materials engineering. A great number of heterogeneous polymer blends have been studied and reported in available literature. A review of empirical knowledge gathered so far is beyond the scope of this basic treatment. Instead, the existing means applicable in projecting polymer blends will be outlined. To reduce experimental time and costs of a blend development, it is highly desirable to have reliable formats for the prediction of considered physical properties, eg, $E_b$, $\sigma_{yb}$, $\sigma_{ub}$, $P_b$. Although modeling and simulations cannot fully replace experimental investigation, their role in the designing and structural analysis of blends is ever increasing.

Physical properties of blends consisting of a continuous matrix and one or more dispersed (discrete) components can be predicted by using adapted models proposed for particulate composite systems (216–220). Most of these models do not consider effects of the particle size, but only of volume fractions of components in the system. Thus, the increase in particle size due to particle coalescence is not presumed to perceptibly affect mechanical properties, except for fracture resistance, which is controlled by particle size and properties of dispersed rubbers. As polymer blends with three-dimensional continuity of two or more components are isotropic materials, simple parallel or series models or models for orthotropic or quasi-isotropic materials are not applicable. Physical properties of blends with partially co-continuous constituents can be calculated by means of a predictive

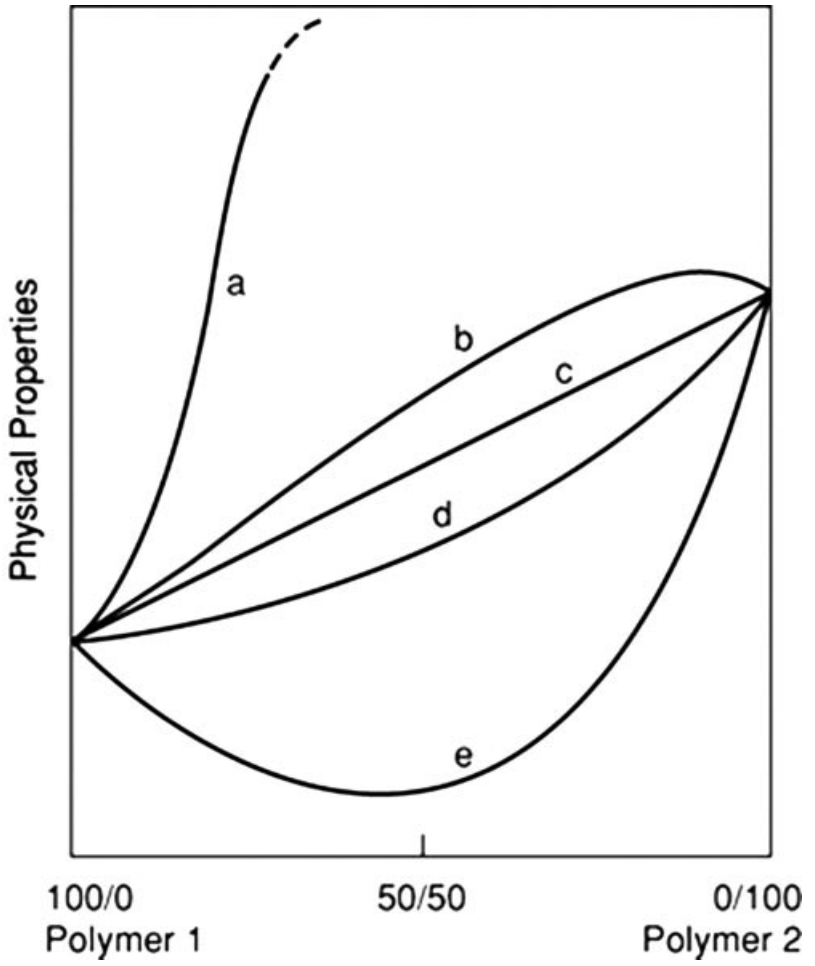


**Fig. 18.** Effect of the composition of heterogeneous binary blends on their physical properties (schematically). (**a**) Fracture resistance, toughness and impact resistance of commercial rubber-toughened polymers; (**b**) modulus and tensile (yield) strength of blends consisting of partially miscible polymers; (**c**) density (straight line corresponds to the rule of mixtures); (**d**) modulus, compliance, tensile yield strength, stress at break, permeability to gases, thermal conductivity of compatible blends with good interfacial adhesion; (**e**) tensile yield strength and stress at break of blends with poor interfacial adhesion; fracture and/or impact resistance of nontoughened blends.

format (221–223) based on a two-parameter equivalent box model (EBM) (Fig. 19) and modified equations rendered by the percolation theory for two-component systems (78,212,224–227). This combination is necessitated by the fact that the EBMs are not self-consistent models. The EBM assumes that either component consists of a fraction continuous in the direction of the acting force ($v_{1p}$ or $v_{2p}$) and a fraction discontinuous in that direction ($v_{1s}$ or $v_{2s}$). In this concept, the lines of force do not cross any interface in the fractions $v_{1p}$ and $v_{2p}$, while the phase continuity is completely disrupted in the fractions $v_{1s}$ and $v_{2s}$, where all

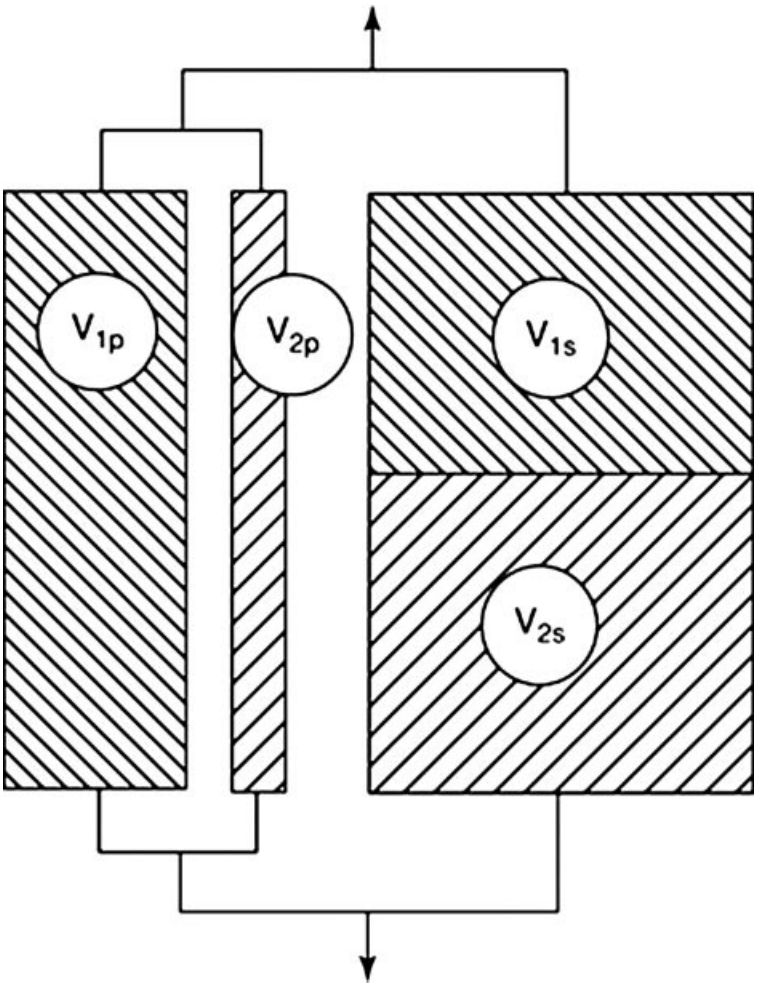


**Fig. 19.** Equivalent box model for a heterogeneous binary blend (schematically).

stress is transmitted through the present interfaces. (Obviously, the continuity of blend components evaluated by means of extraction methods (69,210,228) has a different meaning). The predictive format takes into account (i) the respective properties of components, (ii) the co-continuity interval of components, (iii) interfacial adhesion and (iv) partial miscibility (if any) of components. Application of the EBM to the prediction of physical properties of blends requires (1) calculation the volume fractions $v_{ij}$ and (2) derivation of equations for the properties under consideration in terms of the EBM. Simultaneously predicted physical properties of blends are interrelated because they are calculated by using an identical set of input parameters characterizing a certain phase structure. The model is likely to fail if the blending process produces a significant change in the structure (eg, in crystallinity), and consequently, in the considered properties of one or both constituents.

**Calculation of the Volume Fractions in the EBM.** The EBM is a two-parameter model because out of four volume fractions $v_{ij}$, only two are independent; the volume fractions visualized in Figure 19 are interrelated as follows:

$$\nu_1 = \nu_{1p} + \nu_{1s}; \nu_2 = \nu_{2p} + \nu_{2s}; \nu_1 + \nu_2 = \nu_p + \nu_s = 1 \tag{13}$$

The percolation theory (224–227) provides a universal formula for some physical properties of binary systems (modulus, permeability) where the contribution of the second component is negligible. The formula has been experimentally shown (212,229) to plausibly fit the modulus of model blends with $E_1 \gg E_2$ in the range $v_{1cr} \leq v_1 \leq 1$. Modifying this approach for binary blends, the following equations were derived (221–223):

$$\nu_{1p} = [(\nu_1 - \nu_{1cr})/(1 - \nu_{1cr})]^q, \tag{14a}$$

$$\nu_{2p} = [(\nu_2 - \nu_{2cr})/(1 - \nu_{2cr})]^q \tag{14b}$$

where $q$ is the critical exponent. The remaining $v_{1s}$ and $v_{2s}$ are evaluated by using equation 13. The theoretical critical volume fraction (percolation threshold) $v_{cr} = 0.156$ was calculated (78,219,226,227) for random spatial array of discrete spherical domains. Most reported values of $q$ are located in the interval 1.6–2.0, which complies well with the theoretical prediction (224,227) or $q = 1.8$. In a first approximation, "universal" values $v_{1cr} = v_{2cr} = 0.156$ and $q = 1.8$ can be employed in the EBM, which may provide a good prediction for blends whose components show similar viscosity and elasticity under mixing conditions. Experimental values of $v_{1cr}$ and/or $v_{2cr}$ have usually been found in the interval 0.15–0.25; however, extreme values around 0.03 or 0.46 have also been observed (230). Any considerable change in viscosity of one component influences both $v_{1cr}$ and $v_{2cr}$ (230,231), wherein the component with lower viscosity exhibits a stronger tendency to continuity, which manifests itself in a lower $v_{cr}$ and an asymmetric interval of the phase duality. Owing to enormous complexity, only recently has a quantitative prediction of $v_{cr}$ been attempted (213), which operates with rheological characteristics of components and of the blending equipment. Despite a number of simplifying assumptions, it provides useful guidelines for minimizing $v_{cr}$ of one component in binary blends. In the marginal zone, $0 < v_1 < v_{1cr}$ (or $0 < v_2 < v_{2cr}$), where only component 2 (or 1) is continuous, simplified relations can be used for the minority component in the EBM, ie, $v_{1p} = 0$, $v_{1s} = v_1$ (or $v_{2p} = 0$, $v_{2s} = v_2$), to obtain an approximate prediction of physical properties.

**Moduli of Binary Heterogeneous Blends.** A linear stress–strain relationship, indispensable for modulus measurements, is granted only at very low strains, typically below 1%, where virtually all blends show interfacial adhesion sufficient for transmission of acting stress. At strains exceeding the linearity limit, blend modulus (or compliance) decreases (or rises) with the strain. The tensile modulus of a two-component blend (Fig. 19) is given as (222)

$$E_b = E_1\nu_{1p} + E_2\nu_{2p} + \nu_s^2/[(\nu_{1s}/E_1) + (\nu_{2s}/E_2)] \tag{15}$$

where $v_s = v_{1s} + v_{2s}$. Along with the tensile modulus from stress–strain measurements (Fig. 18, curve d), the storage modulus $E_b'$ and the loss modulus $E_b''$ are frequently used. Dynamic mechanical thermal analysis (DMTA) at a constant frequency is the case of steady state harmonic conditions to which the elastic-viscoelastic correspondence principle is applicable (232). Thus, isochronous DMTA is a method allowing the use of the models for elastic materials also for viscoelastic materials by replacing elastic constants by complex (viscoelastic) counterparts (233,234). Introducing $E_1* = E_1' + iE_1''$, $E_2* = E_2' + iE_2''$ and $E_b* = E_b' + iE_b''$ into equation 15 and separating real and imaginary terms, one obtains

$$E_b' = E_1' v_{1p} + E_2' v_{2p} + v_s^2 N'/M \tag{16a}$$

$$E_b'' = E_1'' \nu_{1p} + E_2'' \nu_{2p} + \nu_s^2 N''/M \tag{16b}$$

where

$$N' = \nu_{1s} E_1' \left(E_2'^2 + E_2''^2\right) + \nu_{2s} E_2' \left(E_1'^2 + E_1''^2\right) \tag{17a}$$

$$N'' = \nu_{1s} E_1'' \left(E_2'^2 + E_2''^2\right) + \nu_{2s} E_2'' \left(E_1'^2 + E_1''^2\right) \tag{17b}$$

$$M = \left(\nu_{1s} E_2' + \nu_{2s} E_1'\right)^2 + \left(\nu_{1s} E_2'' + \nu_{2s} E_1''\right)^2 \tag{17c}$$

A possible occurrence of an additional mechanical transition (loss peak) in the dynamic mechanical spectrum of polymer blends was ascribed to the geometrical arrangement of phases, rather than to a molecular relaxation process within the interfacial area (235).

In boundary regions, ie, $v_1 < v_{1cr}$ or $v_2 < v_{2cr}$, the blend modulus can be calculated from the Kerner – Nielsen equation (216,217,219), which for dispersed component 2 with $E_2 > E_1$ reads

$$E_{b1} = E_1(1 + A_1 B_1 v_2)/(1 - B_1 \psi_2 v_2). \tag{18a}$$

The quantities $A_1$, $B_1$, $\psi_2$ are defined as follows:

(1) $A_1 = (7 - 5\mu_1)/(8 - 10\mu_1)$, where $\mu_1$ is the Poisson ratio of the (glassy) matrix;
(2) $B_1 = (E_2/E_1 - 1)/(E_2/E_1 + A_1)$; $\psi_2 = 1 + [(1 - \nu_{2max})/(\nu_{2max})^2]\nu_2$, where $v_{2max}$ is the maximum packing fraction of the dispersed particles (the value $v_{2max} = 0.63$ for random close packing of monodisperse spheres is usually used (217).

If component 1 with lower modulus $E_1$ is dispersed in a stiffer matrix 2, eg, in rubber-toughened plastics, then inverted relations can be employed (216,217):

$$E_{b2} = E_2(1 - B_2 \Psi_1 \nu_1)(1 + A_2 B_2 \nu_1) \tag{18b}$$

where $A_2 = (8 - 10\mu_2)/(7 - 5\mu_2)$; $B_2 = (E_2/E_1 - 1)/(E_2/E_1 + A_2)$; the formulas for $\psi_1$ and $\psi_2$ are analogous. Alternatively, similar equations derived by other

authors (218,219,236) for particulate systems can be used; the differences in moduli predicted by existing theories are not significant.

**Compliance of Heterogeneous Binary Blends.** As end products made of thermoplastics and their blends are frequently exposed to a long-lasting dead load, their resistance to creep becomes a significant characteristic of their dimensional stability. By introducing a co-continuous creep-resistant component, the creep of blends can be substantially reduced. To anticipate the time-dependent compliance $D_b(t)$ of a blend, the corresponding functions $D_1(t)$ and $D_2(t)$ of the components are to be experimentally evaluated. In analogy to the blend modulus (Fig. 18, curve d), the compliance of heterogeneous binary blends with co-continuous components reads (237–239):

$$D_b(t) = \left\{v_{1p}/D_1(t) + v_{2p}/D_2(t) + (v_{1s} + v_{2s})^2/[D_1(t)v_{1s} + D_2(t)v_{2s}]\right\}^{-1} \tag{19}$$

To describe the compliance of blends with one continuous component and one discontinuous component, equation 19 can provide a first approximation by using $v_{1p} = 0$, $v_{1s} = v_1$ or $v_{2p} = 0$, $v_{2s} = v_2$. More accurate equations can be obtained by modifying existing equations (213). If the minority polymer 2 of the volume fraction $v_2$ having a lower compliance $D_2(t) < D_1(t)$ is dispersed in polymer 1, the compliance $D_{b1}(t)$ of the blend is (237)

$$D_{b1}(t) = D_1(t)[1 - B_1(t)\psi_2 v_2]/[1 + A_1 B_1(t) v_2] \tag{20a}$$

where $B_1(t) = [D_1(t)/D_2(t) - 1]/[D_1(t)/D_2(t) + A_1]$; $A_1$ and $\psi_2$ are defined for equation 18a. If the component 1 is dispersed in the component 2, then the inverted relation applies:

$$D_{b2}(t) = D_2(t)[1 + A_2 B_2(t) v_1]/[1 - B_2(t)\psi_1 v_1] \tag{20b}$$

where $B_2(t) = [D_1(t)/D_2(t) - 1]/[D_1(t)/D_2(t) + A_2]$; $A_2$ and $\psi_1$ are defined for equation 18b.

As the stress–strain linearity limit of most thermoplastics and their blends is very low, nonlinear viscoelastic behavior of heterogeneous blends needs to be considered in most cases. The nonlinearity is at least partly ascribed to the fact that the strain-induced expansion of materials with Poisson's ratio smaller than 0.5 markedly enhances the fractional free volume (240). Consequently, the retardation times are perpetually shortened in the course of a tensile creep in proportion to the achieved strain. Thus, knowledge of creep behavior over appropriate intervals of time and stress is of great practical importance. The handling and storage of the compliance curves $D(t,\sigma)$ in a graphical form is impractical, so numerous empirical functions have been proposed (241), eg,

$$D(t,\sigma) = W(\sigma)(t/\tau_{rm})^n \tag{21}$$

where $W(\sigma)$ is a function of the stress, $\tau_{rm}$ is the mean retardation time, and $0 \leq n \leq 1$ is the creep curve shape parameter reflecting the distribution of retardation times. Parameters characterizing the nonlinear compliance of the parent polymers

can be extracted from generalized creep dependencies obtained by means of time-strain superposition. The predictive format based on equations 14a, 14b, 19 and 21 allows the prediction of corresponding parameters for blends and the construction of the creep curves of blends for selected stresses in the region of recoverable stress-strain behavior (238,239).

**Yield and/or Tensile Strength of Heterogeneous Binary Blends.** If blend components show yielding (usually at a strain of 3–6%), the yield strength in tension $\sigma_{yb}$ of the resulting blend obeys the following equation, derived in terms of the EBM in Fig. (19) (221,242):

$$\sigma_{yb} = \sigma_{y1}\nu_{1p} + \sigma_{y2}\nu_{2p} + A\sigma_{y1}\nu_s, \tag{22}$$

where $\sigma_{y1} < \sigma_{y2}$ characterize the parent polymers and $0 \leq A \leq 1$ the extent of interfacial debonding. Two limiting values of $\sigma_{yb}$, identified with the lower or upper bound, can be distinguished by means of equation 22: (i) Interfacial adhesion is so weak that complete debonding occurs before yielding between the fractions of constituents coupled in series ($A = 0$ at the yield stress). As a function of blend composition, the lower bound of $\sigma_{yb}$ passes through a minimum (Fig. 18, curve e). (ii) Interfacial adhesion is strong enough to transmit the acting stress between constituents so that no debonding ($A = 1$) appears in the course of yielding; then the contribution of the series branch in the EBM is added to that of the parallel branch (the effect of different strain rates in the parallel and series branches on $\sigma_{y1}$ and $\sigma_{y2}$ is neglected). However, if two components differing in the yield strength are coupled in series, then this branch yields at $\sigma_{y1}$ or $\sigma_{y2}$, whichever is lower. The upper bound of $\sigma_{yb}$ is a monotonic function of the blend composition (Fig. 18, curve d). Whenever a partial or complete debonding occurs before yielding, then $\sigma_{yb}$ passes through a minimum as a function of blend composition (211). A good correlation was found between the partial miscibility of blend components and their interfacial adhesion (243).

The yield strength $\sigma_{yb1}$ of particulate systems, where dispersed particles do not yield and have a good adhesion to the matrix, is approximately equal to that of the matrix $\sigma_{y1}$ (244). In the case of "zero" adhesion, the yield strength $\sigma_{yb2}$ drops with the volume fraction of particles (219,245):

$$\sigma_{yb2} = \sigma_{y2}\left[1 - (\nu_1/\nu_{1max})^{2/3}\right] \tag{23}$$

The latter formula also holds for glassy matrices with rubber-like inclusions, because yield strength of the dispersed component is negligible (219).

With regard to the experience that equation 23 is suitable for the evaluation of the yield as well as tensile strength of particulate systems, equation 22 can also be tentatively applied (221–223) for the tensile strength $\sigma_{ub}$ of blends by replacing the yield strengths $\sigma_{y1}$ and $\sigma_{y2}$ by the tensile strengths $\sigma_{u1}$ and $\sigma_{u2}$, respectively. If fracture mechanisms in the blend components are very different, the format may not fit the $\sigma_{ub}$ versus $v_2$ dependence.

**Application of the Predictive Formats.** In addition to the prediction of selected physical properties of envisaged blends, subsequent comparison of model calculations with experimental data allows the experimentalists (i) to analyze the phase structure of prepared blends, (ii) to evaluate interfacial adhesion or the

extent of interfacial debonding, and (iii) to assess to which extent the potential of a material has been exploited, etc. A great advantage of the EBM approach is that several physical properties can be simultaneously evaluated, eg, modulus, yield, or tensile strength, and permeability to gases (222,223,246). If no information is available about the phase structure of blends, the properties can be predicted by using the "universal" values $v_{1cr} = v_{2cr} = 0.16$ and $q = 1.8$. However, this should be regarded as a first approximation that may not well approximate experimental data due to the fact that $v_{1cr}$ and $v_{2cr}$ of a studied system may be different, being affected by the relative viscosities of components, conditions of blend mixing, phase structure coarsening, etc. Conversely, as soon as some experimental data for a specific system are available, it is possible to determine actual $v_{1cr}$ and $v_{2cr}$ by a fitting procedure; thus the formats can be alternatively viewed as an efficient tool for analysis of the phase structure of blends. In a similar way, the phase structure of ternary blends (242,247) and/or the extent of interfacial debonding (248) can be evaluated. The outlined format for the modulus was successfully used in the structure analysis of interpenetrating epoxy and silica networks (249). Blends consisting of partially miscible polymers often show positive deviations (Fig. 18, curve b) of the moduli and yield strength, (250,251) which are ascribed to two effects: (i) respective properties of one or both conjugate phases are higher than those of parent polymers; (ii) molecular mobility in conjugate phases is reduced due to associative interactions (heterocontacts) between the chains of components. The properties of these blends can be modeled by combining the predictive formats with an empirical equation expressing the composition of conjugate phases as a function of blend composition (251). The predictive format was also used for manifestation of the effects of the phase structure coarsening (narrowing of the co-continuity interval) on the modulus, yield or tensile strength, and gas permeability of heterogeneous polymer blends characterized by good or poor interfacial adhesion (252). If postmixing treatments (quiescent annealing before freezing-in the melt, molding, reprocessing) account for a more profound drop in blend properties, then it is likely that—in addition to phase structure coarsening of the blend—the respective properties of constituents have deteriorated due to changes in their structure or due to chemical degradation.

**Toughness of Polymer Blends.** Toughness (fracture resistance) ranks among the most closely watched properties of polymer materials because it is an important prerequisite in most applications. It is commonly defined as the ability to resist fracture by absorbing mechanical energy (253–256). In general, toughness is an extremely complex phenomenon, depending on polymer composition (molar mass, chain flexibility, chain-entanglement density), surface energy, density, crystallinity, modulus, and yield strength as well as on testing conditions (specimen geometry and dimensions, mode of loading, strain rate, temperature, presence of notches, etc.). Only parameters based on fracture mechanics can separate the effects of testing conditions from the effects of intrinsic material properties. Relevant material characteristics can be derived from either the energy balance approach or the stress intensity approach. Linear elastic fracture mechanics (LEFM), which is appropriate for (semi)brittle materials, operates with the strain energy release rate and the stress intensity factor. Nonlinear fracture mechanics (257,258) developed for ductile materials—including toughened polymers and blends—has introduced the J-integral fracture toughness, which can be

considered as a nonlinear elastic energy release rate. A widely used method is that of the essential work of fracture (EWF), which is a material property related to the J-integral (255). Despite an enormous amount of empirical knowledge gathered so far, there are no quantitative means for anticipating the toughness of new materials.

Amorphous glassy polymers show two types of localized deformation mechanisms, ie, crazing and shear yielding (256,259–261). A craze can be described as a microcrack bridged by polymer fibrils (5 – 20 nm in diameter) partially bearing the load. Crazes initiated by pre-existing defects or flaws typically develop in a plane perpendicular to a maximum principal stress in polymers, whose crazing stress is lower than yield stress (under the conditions of testing) (262–264). Crazing involves formation of microvoids that account for an increase in volume. Crazes grow through drawing of fibrils formed from the bulk polymer, and at the final stage give rise to cracks at a stress below that necessary to cause bulk shear yielding. The energy absorption per unit volume is relatively high within the craze deformation zone, but the amount of material involved in that absorption is very limited, so ensuing brittle fracture requires a very low mechanical energy. Brittle polymers have a low crack initiation energy (unnotched toughness) as well as a low crack propagation energy (notched toughness) (265). Brittle fracture is typical of PS, SAN, PMMA and highly crosslinked glassy polymers (256,259,260).

Shear yielding involves localized or homogeneous plastic deformation occurring without any volume change. A number of glassy polymers possess some degree of ductility (at room temperature) at moderate rates of straining, eg, polycarbonate (PC), polysulfone, and polyethersulfone (260). Ductile fracture requires sufficient molecular (segmental) mobility for shear yielding (plastic flow) to occur. Yielding localized in planar zones with high shear strains gives rise to "shear bands" at an angle of about 45° to the acting force, ie, in the direction of maximum shear stress. The strain hardening due to chain orientation eventually imposes a limit of the achievable plastic deformation. Ductile behavior is favored by uniaxial stress conditions, low strain rates, elevated temperature and smaller specimen cross-section (256,260). Ductile polymers have high crack initiation energy and low crack propagation energy (265,266). The transition between crazing and shear yielding is mainly predetermined by the entanglement and/or crosslinking density, because an increasing network density hampers the void formation in the process of crazing. Thus, the craze initiation stress is lower than the shear band initiation stress, and crazing prevails in polymers with a network density lower than a critical value. Shear yielding is typical of highly entangled thermoplastics with flexible chains.

In semicrystalline polymers, the main energy-absorbing mechanism is shear yielding (261,267,268). Local crazing may take place as a part of the fracture process ahead of a running crack without being an important energy-absorbing mechanism. Semicrystalline polymers usually have high toughness at temperatures above their $T_g$. Their toughness decreases with increasing crystallinity and perfection of the crystallites because shear yielding is impeded. Rising spherulite size has negative effects on toughness because larger defects and voids are created, and cracks propagate more easily along the interfaces between coarser spherulites. Higher molar mass accounts for the enhanced number of tie molecules between crystallites and spherulites, which improve the fracture resistance (260).

Molecular mobility, crazing, and shear yielding are thermally activated rate processes that follow the Eyring equation (256,264). For this reason, all plastics are brittle under extreme testing conditions (low temperatures and high strain rates permit only crazing because the yield stress is higher than the craze initiation stress). The brittle/ductile transition temperature $T_{b/d}$ of a polymer means that at $T < T_{b/d}$ the fracture is brittle, while at $T > T_{b/d}$ the fracture is ductile. The transition is a consequence of the fact that the yield strength decreases faster with rising temperature than the brittle strength so that yielding starts to be a dominating deformation mechanism at $T > T_{b/d}$. This temperature, which is of major engineering importance, always lies below $T_g$. However, it increases with the strain rate, crosslinking density, presence of notches, etc. (264).

Advanced characterization of the fracture processes in polymers and their blends is provided by the methods of fracture mechanics. Comprehensive reviews of this topic can be found in References 253, 255–259. Despite the achieved progress in this field, the plastics industry traditionally employs standard empirical tests for evaluating toughness (259,269). The Charpy or Izod impact test and falling-weight impact tests are widely used, although they provide only a semiquantitative basis for selection of materials. The impact resistance is a measure of the ability of a material to withstand the application of a sudden load without failure (259); however, it is not a material property because it depends on testing method and conditions, specimen geometry, and other factors. The obtained values are suitable for simple ranking of available materials or for evaluation of achieved improvements in material formulations. It should be noted that it is extremely difficult to correlate the impact strength found for a type of specimen with the impact performance of the manufactured article (260). In practice, it is advisable to select a method and testing conditions resembling the service conditions. Instrumented impact devices, which register the load-displacement curves in the course of impact, provide a deeper insight into the fracture mechanisms.

Toughening of rigid polymers consists of the involvement of their large fractions in energy absorption processes. To achieve this goal, a suitable amount of rubbery particles (of proper size, modulus, crosslinking density, and interfacial adhesion) is to be evenly dispersed in the brittle matrix to function as stress concentrators and to initiate multiple energy-absorbing plastic microdeformations. A good dispersal of rubbery component and formation of an optimum size of particles are often aided by suitable compatibilization. During initial deformation, cavitation (formation of voids of the order of 10 nm) occurs within or around the rubber particles, which triggers either multiple crazing, in polymers prone to crazing, or shear deformations (bands) in shear-yielding matrices (256). Cavitation is an essential step in the toughening process because it relieves the triaxial tension built up in the proximity of the crack tip. After cavitation, only biaxial tension remains, which is more favorable to shear yielding. A spectacular upswing in the toughness occurs at a certain rubber volume fraction, which indicates a percolation character of the underlying process. In this way, the toughness can routinely exceed by 1–2 orders of magnitude the value characterizing a neat rigid matrix (Fig. 18, curve a). However, in practice there is always a need to balance fracture resistance against other properties, eg, stiffness, resistance to creep, and dimensional stability.

As the optimum fraction of the rubber component is rather low (0.05–0.30), the term “rubber-toughened polymers” (instead of “blends”) is commonly used.

Almost any engineering plastic can be made tougher in its rubber-modified version, but at the expense of modulus and yield strength. Although the mechanism of plastic deformation in such materials depends on the properties of matrix (molecular weight, crystallinity, entanglement density, cohesive energy), dispersed rubber (modulus, cohesive energy, particle size, crosslinking), and adopted test conditions (test specimen dimensions, test speed, test temperature, notch dimensions), the fracture resistance of toughened polymers is primarily derived from the deformation and failure behavior of the rigid matrix, where most of the mechanical energy is absorbed via multiple crazing and/or shear yielding during straining and fracture. Semicrystalline polymers usually fracture in a ductile manner due to high resistance to crack initiation; however, in the presence of a sharp defect (notch) they show brittle fracture, because their resistance to crack propagation is low (255). For this reason, impact resistance of the notched test specimens is an important criterion of the achieved toughening. The quantitative theory of toughening based on the energy balance model (270) correctly predicts trends in the deformation and fracture behavior of toughened plastics with various structures. However, due to extreme complexity of the toughening phenomenon, there has been no format for the prediction of fracture resistance of rubber-modified plastics to date.

Rubber particle cavitation and subsequent multiple matrix crazing is the dominant mechanism of toughening in rubber-modified brittle matrices such as HIPS, SAN, PMMA, and ABS polymer (260,271,272). In less brittle matrices, such as SAN and PMMA, mixed crazing and shear yielding can occur (265). In the beginning, application of external stress causes the biggest rubber particles to cavitate and initiate the first series of crazes, which grow by increasing their area and thickness. The rising deformation initiates secondary cavitation of smaller rubber particles and further crazing. Thus, crazes lying close to a craze plane begin to connect together; a rapid craze thickening follows, involving the drawing of fresh polymer from the walls of rising crazes. The latter stage can be identified with an effective energy-consuming process. Fibrillation occurs in an increasing fraction of rubber particles, which stretch in parallel with the crazes up to a saturation point. The rupture of a blend deformed by multiple crazing is assumed to be associated with failure in the fibrillated rubber particles when the local tensile strain exceeds their limiting value. The light scattering from microvoids formed in the matrix crazes and/or in the rubber particle cavities accounts for the stress whitening (273).

In HIPS, where the "salami" rubber particles consist of hard polystyrene subinclusions embedded in the matrix of crosslinked rubber, a specific type of cavitation was revealed (256). Cavitation in the rubber "membranes" results in a craze-like structure where rubber fibrils form bridges between the PS subinclusions and between the subinclusions and the PS matrix. Yielding in the matrix allows the rubber fibrils to stretch and the rubber particles to expand until strain hardening stops the process. PVC and poly (oxymethylene) (POM) also show very high values of the notched Izod toughness when the incorporated rubber forms an intermeshed (network) structure (265) instead of discrete particles. A higher effectivity of intermeshed rubber phase morphology was ascribed to a lower percolation threshold in comparison with that for an assembly of spherical particles. The toughening mechanism of ABS consists in the formation of numerous shear

bands in addition to massive crazing (259). A similar effect can be produced in SAN by bimodal-sized rubber particles (265).

Shear yielding is the process by which most intrinsically ductile polymers achieve high strains. The incorporation of a rubbery component still enhances the toughness so that supertough materials can be produced (260,265,274), but the main purpose of the modification is to improve the resistance to crack propagation (notch sensitivity) (259). The high stress concentrations generated in the matrix by rubber particles bring about a spectacular rise in the rate of plastic deformation, because the adjacent matrix is free to yield and stretch in the way that was not possible in the neat matrix. The main factors controlling the shear yield stress of toughened plastics are the yield behavior of the rigid matrix and the volume fraction, shear modulus, and particle size of the dispersed rubber. Essential gains in toughness are achieved only when the cohesive failure within the rubber particles induces accelerated shear yielding in the matrix, which is then followed by strain hardening of the yield zone due to stretching of both rubber and rigid matrix. In this plastic deformation process, chain segments slip past each other, so that the material in the yield zone changes its shape, while only minor changes in density are due to disturbed molecular packing. Yielding localized in planar zones with high shear strains gives rise to pronounced shear bands; strain hardening due to the chain orientation eventually imposes a limit of the achievable plastic deformation. Toughening is particularly effective in the case of an array of closely spaced rubber particles, which assures that the ligaments between particles become fully yielded (256). The maximum degree of macroscopic toughness can be achieved if the local ligament thickness (surface-to-surface interparticle distance) decreases below its critical value (261,266), which is related to the experimental finding that brittle polymers become ductile below a critical specimen thickness (less than 1 $\mu$m). The critical ligament thickness is characteristic of the matrix for a given loading mode, temperature, and rate of deformation (266).

Toughness of semicrystalline polymers is enhanced by means of techniques similar to those developed for glassy polymers (260,267,275). Rubbery particles usually initiate both massive crazing and shear banding, which depend on blend composition, morphology, rubber particle size, and interfacial adhesion. An additional positive effect of the rubber component may consist in that its nucleating effect leads to finer spherulitic structure, thus improving the inherent toughness of the crystalline phase. Specific nucleating agents can markedly increase the toughness of the PP matrix by modifying crystalline structure and increasing the concentration of tie molecules (276,277).

Because of profound differences in the deformation and fracture behavior of polymer matrices, the optimum size of toughening rubber particles depends on the inherent fracture mechanism of a matrix. On the other hand, these optimum dimensions are affected by some properties of the rubber used, eg, modulus, viscosity, and crosslinking density. Rubber particles of improper size are ineffective in the toughening process. The existence of a minimum particle size for efficient toughening corresponds to the minimum particle size required for cavitation (256). Extensive experimental work has established that the particle size of a toughener should lie within an optimum range. The optimum diameter of rubber particles for efficient toughening of brittle glassy polymers tending to craze decreases with their entanglement density; the values reported (265) for PS, SAN, and PMMA

are 2.5, 0.75, and 0.25 $\mu$m, respectively. On the other hand, matrices absorbing fracture energy via shear yielding (polycarbonate, polyamides, PET, PBT, PVC) are commonly toughened with particles of 0.5 $\mu$m or less, eg, 0.2–0.3 $\mu$m for polyamides, added in the amounts necessary for the critical interparticle distance. The critical ligament thickness in a matrix depends on temperature, strain rate, loading mode, and other factors (265). Thermoset resins are routinely toughened by liquid carboxy-terminated butadiene rubbers (CTBN) dissolved in the resin mixture, and after curing, form separate domains 0.2 – 0.5 $\mu$m in diameter (253).

A fine dispersion of rubber in a polymer matrix is facilitated by a low interfacial tension between blended components in the molten state. Under these conditions, the rubber particles may not be well bonded to the matrix for efficient stress transfer (54). At any rate, the final particle size strongly depends on the rubber relative viscosity and blending conditions. The goal of concurrently optimizing dispersion and adhesion of a rubbery modifier is rather difficult to achieve. An elegant solution is offered by core-shell impact modifiers with a well-defined size and a narrow particle-size distribution (278). A major advantage of core-shell particles is that their size is set during their synthesis (emulsion polymerization) and remains the same after the dispersal in a host matrix. A soft core, made up of a rubbery polymer, is surrounded by a shell of grafted rigid polymer. The core of the particles provides the soft component that induces toughening mechanisms. The shell of a much higher $T_g$ than the core has two primary functions: (i) to facilitate isolation of the particles from emulsion and to keep the cores from adhering to one another; (ii) to act as the interlayer binding the matrix to the core. Core-shell particles of acrylate rubber-PMMA, polybutadiene-PMMA, or polybutadiene-SAN are used for PA, PET, and PBT; ABS core-shell materials are effective in toughening PBT and PC. The amount of incorporated modifier particles varies from 5 to 30% by weight of the matrix.

A key factor in the performance of core-shell particles as impact modifiers is their adhesion to the host matrix, determined by the composition of both shell and matrix (278). If the latter polymers are compatible (miscible or partly miscible), the toughener will be effective. However, in most cases, the matrix and shell consist of dissimilar polymers. Also in this situation, solubilization of the matrix polymer into the grafted shell needs to be ensured to develop proper interfacial adhesion. High degrees of solubilization are favored by negative values of the interaction energy density, high molecular weight of the shell relative to the matrix, and a low shell thickness. If the matrix and shell are highly incompatible, introduction of a suitable compatibilizer can enhance the efficiency of core-shell impact modifiers. Alternatively, the matrix/shell adhesion can be enhanced by employing possible reactions between functional groups introduced in the shell and reactive sites of the matrix. Recent advances in polymerization techniques permit synthesis of various types of modified polyolefins (279), eg, polypropylene toughened with evenly distributed particles of ethylene-propylene rubber bound to the matrix.

The transition of dispersed particles from the rubbery to glassy state defines the lowest temperature at which the incorporated rubber is able to reduce the matrix yield stress and account for significant toughening (280,281). The effect of added rubber usually fades away at temperatures 10–20 K above its $T_g$, which is manifested as a sharp drop in the fracture energy (256). An equation was derived for the brittle-ductile transition temperature as a function of the particle

volume fraction, size, distribution, and matrix ligament thickness (282). However, this critical temperature is also affected by testing conditions. In proportion to their fraction, rubbery impact modifiers reduce the modulus and yield strength of toughened polymers as quantified by equations 18b and 22, respectively.

Impact resistance of ductile polymers was also improved by blending with 5–15% of a brittle component, eg, polycarbonate with SAN (283) or polyamide 6 with poly(styrene-*co*-maleic anhydride) (SMA) (284). Although the enhancement of impact resistance is lower than in the ductile matrix/rubber systems, the advantage of rigid particles is a simultaneous increase in toughness and stiffness. To achieve these effects, brittle inclusions should be small and interfacial adhesion should be high. Then, the brittle inclusions having a sufficiently higher modulus and a lower Poisson's ratio than the matrix become ductile under the action of the compressive component of stress (285,286) and absorb mechanical energy. To prevent formation of a co-continuous brittle component at higher volume fractions, it is convenient to add two brittle and incompatible minority components. To achieve their separate dispersion, the surface energy of one minority component should be higher than that of the matrix, while the reverse relation holds for the other minority component (242). Ternary blends of polyamide 6 containing rigid particles of SMA (about 5%) and particles of maleated ethylene-propylene rubber (about 5%) are an example of blends with balanced mechanical properties (286,287). In these blends, the losses in stiffness and tensile strength caused by rubbery component are (more than) compensated by the action of the brittle component, while both minority components contribute to the toughness enhancement.

Recently, specific conditions have been elucidated under which isometric filler particles (calcium carbonate) can account for a considerable toughening of PE (288) and PP (289). The notched Izod impact energy of PE/$CaCO_3$ materials rose by one order of magnitude when the mean interparticle ligament thickness of the PE matrix dropped to values below 0.6 $\mu$m. Under these conditions, the stiff filler brought about a substantial increase in both the modulus and toughness. The achieved improvements of the toughness of PP/$CaCO_3$ were smaller, while polyamide 6/$CaCO_3$ (290) showed brittle behavior, probably due to a high plastic resistance of the matrix. In all cases, dispersal of fine filler particles and elimination of their agglomerates were critical for enhancing the toughness.

**Rheological Properties of Molten Blends.** The dependence of shear viscosity, first normal stress difference or storage modulus on blend composition varies very substantially from system to system. According to the type of relation between the logarithm of viscosity and concentration, blends were classified into four categories (291–293). Additive blends fulfill the log-additivity rule:

$$\log\eta = \sum_i v_i \log \eta_i \tag{24}$$

where $v_i$ and $\eta_i$ denote, respectively, volume fraction and viscosity of the component $i$. Other categories are blends showing a positive deviation from log-additivity, blends with a negative deviation, and blends where both the positive and negative deviation have been observed. Because polymer blends are non-Newtonian liquids with $\eta$ dependent on $\dot{\gamma}$, dependences of $\eta$ on the blend composition determined at a constant shear rate and at a constant shear stress can be different. Dependences

at a constant stress are more plausible, because the stress is continuous at the interface in contrast with the deformation rate. Different types of the dependence of $\eta$ on $v$ at different shear stresses were found for some systems (291). Therefore, the above classification does not characterize polymer pairs only, but it is also a function of flow conditions. Dependences of the first normal stress difference and storage modulus on blend composition are similar to those for viscosity (291).

Generally, there is interrelation between rheological properties and morphology of flowing blends. Therefore, the morphology must be assumed in calculation of rheological properties or both characteristics must be calculated simultaneously. Great attention has been paid to the development of the theory of viscosity for blends containing a small amount of a dispersed component (96,291,292). A number of expressions for viscosity were derived using various approximations for these blends. For blends containing a very small volume fraction, $v$, of Newtonian droplets in the Newtonian matrix, the following equation was derived for $C_a \ll 1$.

$$\eta = \eta_m\left(1 + \frac{5p+2}{2p+2}v\right) \tag{25}$$

Equations considering somewhat higher contents of dispersed droplets, higher $C_a$ and viscoelasticity of the components were derived. Also, these expressions predict for blends containing dispersed droplets that viscosity of a blend is higher than that of its matrix also for $p \ll 1$. This is a general feature of all theories describing rheological properties of dispersed droplets in matrix and assuming stick condition at the interface.

The Palierne model (294,295) describes a linear viscoelastic response of a dispersion of droplets that are spherical in stress-free state. The model may account for viscoelastic properties of both matrix and droplets, effects of finite concentration, distribution of size and composition of the droplets, and interfacial tension effects (also for compatibilized blends). The agreement of its predictions with experimental results is good (295). Description of rheological properties of blends with co-continuous structure is more complicated. In this case, it is useful to characterize the interface. The interfacial area per unit volume $Q$ and specific anisotropy tensor $q$, characterizing anisotropy of the microstructure are used as proper characteristics for blends with a general shape of the interface (96). Development of theories for prediction of time evolution of $Q$ and $q$ and average stress tensor, which would serve for prediction of rheological properties, is in progress (96).

A reasonable explanation of negative deviation of $\eta$ from log-additivity rule (eq. 24) was proposed by Utracki (293). It is assumed that the interlayer slip at the interface should be considered in immiscible polymer blends. A semiempirical theory considering the emulsion behavior and interlayer slip factor can predict all the above-mentioned categories of blend behavior with respect to log-additivity rule depending upon the system parameters. More recently, the origin of the slip at the interface was discussed in more detail (296). Suppression of the slip at the interface by the presence of a compatibilizer can explain the typically observed higher viscosity of compatibilized blends than that of the related blends without compatibilizer (297). Most polymer blends have the dependence of shear viscosity on the shear rate similar to that of homopolymers only with a somewhat shorter

Newtonian plateaus due to the effect of the interface (291,295). In contrast, dynamically vulcanized blends show yield stress, ie, a strong increase in $\eta$ with decreasing shear rate in the region of low $\dot{\gamma}$ (298–300). It seems that the yield stress is induced by long-living entanglements between crosslinked domains of characteristic size of about 1 $\mu$m.

**Permeability of Blends to Gases and Vapors.** The permeation of gases, vapors, and liquids through films (layers, walls) of blends is of primary importance in many applications (packaging, pipes, tanks, etc.). The permeability of polymers is mainly determined by their polarity and crystallinity. Polyolefins are good barriers to moisture, but are highly permeable to hydrocarbons. On the other hand, aliphatic polyamides have outstanding resistance to hydrocarbons, but poor resistance to moisture. Thus, there are many reasons for blending various polymers to tailor materials with balanced and acceptable physical properties (301).

For a miscible polymer pair, the blend permeability $P_b$ was empirically found to approximately obey the semilogarithmic additivity rule (302):

$$1nP_b = \nu_1 1nP_1 + \nu_2 1nP_2 \tag{26}$$

where $P_1$ and $P_2$ are the permeabilities of components. In the free volume approach (303,304), it is assumed that the free volume of the mixture consists of the additive contributions from each component, which leads to the following equation:

$$\ln(P_b/Q) = [\nu_1/\ln(P_1/Q) + \nu_2/\ln(P_2/Q)]^{-1} \tag{27}$$

where $Q$ is a characteristic constant for the gas. The transport through blends consisting of miscible polymers is comprehensively reviewed in References 301–303.

Heterogeneous blends of immiscible or partially miscible polymers are much more important engineering materials than homogeneous blends. The permeability of blends consisting of a continuous matrix and dispersed particles of another polymer can be approximated by models developed for particulate systems (301,302). However, these models (assuming dispersed components in the form of spheres, cylinders, cubes, lamellar structures of random orientation, etc.) were found inadequate for the prediction of the blend permeability throughout the composition range (225,305–307), a part of which necessarily corresponds to blends with co-continuous components. Thus, the EBM (Fig. 19) combined with the percolation approach was found (301) to be the most convenient predictive model for the permeability of heterogeneous blends. The permeability of binary blends consisting of partially continuous components can be predicted (223,230,308) using the format formally analogous to that for tensile modulus given in the previous section on mechanical properties (Fig. 18, curve d):

$$P_b = (P_1 v_{1p} + P_2 v_{2p}) + v_s^2/[(v_{1s}/P_1) + (v_{2s}/P_2)] \tag{28}$$

The data are usually presented as the relative permeability $P_{br} = P_b/P_1$ (relative to the component 1 with a lower permeability) versus blend composition. The "basic" curve calculated for $v_{1cr} = v_{2cr} = 0.16$ and $q = 1.8$ by means of equations

14 and 28 may deviate from experimental data if component 2 with a higher permeability, which controls $P_{br}$, is characterized by $v_{2cr}$ different from 0.16. *Vice versa*, it is possible to evaluate realistic values of $v_{1cr}$ and $v_{2cr}$ in individual series of blends by fitting experimental data. For blends consisting of components that differ by 2–4 orders of magnitude in their permeability, the semilogarithmic plot is more instructive (308); moreover, it indicates $v_{2cr}$ as a break (discontinuity), so that $v_{2cr}$ can be adjusted with an accuracy of about 0.01. In this way, the format becomes an efficient tool for the analysis of the phase structure of polymer blends. In marginal regions $0 < v_1 < v_{1cr}$ (or $0 < v_2 < v_{2cr}$), simplified relations can be used for the EBM, ie, $v_{1p} = 0$, $v_{1s} = v_1$ (or $v_{2p} = 0$, $v_{2s} = v_2$), to obtain an approximate prediction of permeability. The permeability of layered materials can be modeled as the series coupling of components.

The outlined format was found to match up well the permeability of a number of permeant-blend systems, eg, water–HDPE/LDPE, toluene–HDPE/polyamide 6, methanol–polyethylene/silicone rubber, oxygen–PVC/chlorinated PE (230); oxygen–PMMA/siloxane copolymer, oxygen–PE/poly (vinylidene chloride), oxygen–poly(ethylene-*co*-vinyl alcohol)/poly(ethylene-*co*-vinyl acetate) (308). The agreement with experimental data was very good throughout the composition range. Moreover, the format is suitable for simultaneous prediction or fitting of several physical properties, such as modulus and permeability (246) or modulus, tensile strength, and permeability (223).

## Commercially Important Polymer Blends

There are three practical reasons for blending of polymers: (i) developing materials with desired properties, (ii) extending performance of expensive polymers by diluting it with a low cost polymer and (iii) utilizing plastic scrap by mechanical recycling. It is estimated that about one third of all commercially produced polymer materials are blends of two or more polymers. These multicomponent and largely multiphase materials show various combinations of properties unattainable in any one polymer alone. Major concern is focused on increasing impact strength, processability, tensile strength, stiffness, and heat resistance (309). It should be emphasized that an improvement in one property leads usually to deterioration of another property, and therefore the main efforts have been devoted to attaining well balanced properties of the final material required for the pertinent applications. Commercially produced polymer blends are the subject of several excellent monographs (1,55,56,310–312). Thus, only several examples of technically important polymer blends prepared by different compatibilization procedures are briefly presented in this chapter together with basic information on the recycling of mixed plastic waste.

**High Impact Polystyrene (HIPS).** Polystyrene shows excellent processability, good appearance, tensile strength, and thermal and electrical characteristics; however, its brittleness considerably limits its use in high performance products. Therefore, modification of its toughness made possible rapid growth of high impact polystyrene grades (60,272,313). Polystyrene whose impact strength is modified by the incorporation of rubber can be manufactured either by

mechanical blending of components under controlled conditions or by grafting of the polymerizing styrene onto the rubber.

Mechanical blending of PS with PB is not very effective, and in its classic form is a matter of the past. Blending technology is still used for modification of polystyrenes with special rubber components such as thermoplastic elastomers, eg, SBS or SEBS. HIPS is also sometimes blended with styrene homopolymer to yield material with reduced cost but intermediate properties still acceptable for some applications.

At the present time, HIPS is produced by polymerization of styrene containing 5–10% of dissolved polybutadiene. The process yields both the styrene homopolymer and the polybutadiene-*graft*-polystyrene, where PS side chains are grafted onto the main polybutadiene chain. The process can be carried out technologically as mass (bulk) polymerization or as a mass suspension process, either batchwise or continuously. It is initiated thermally or by suitable initiator (such as dibenzoyl peroxide). As conversion reaches 2–3%, phase separation occurs as a result of immiscibility of PS and PB. The system forms so called polymeric oil-in-oil emulsion, in which the dispersed phase is a solution of PS in styrene, and the continuous phase is a solution of PB in styrene. Grafted copolymer is formed at the interface and acts as an emulsion stabilizer. As the volume ratio of PS and PB in styrene approaches one, and the mixture is subjected to sufficiently strong shearing agitation—phase inversion takes place. Sufficient agitation of the reaction mixture in the phase inversion region is essential for morphology control of the final polymer blend. Particles of newly formed dispersed phase still contain permanently included residues of the original dispersed styrene phase as isolated particles. The presence of polystyrene subinclusions in polybutadiene particles is characteristic of HIPS, increasing its impact strength due to an increase in the "effective volume" of the PB phase. Near the completion of polymerization, crosslinking of the rubber component takes place. Rubber crosslinking must be sufficient to prevent disintegration during processing.

The HIPS performance is controlled by the amount and type of rubber, particle size distribution, rubber-phase volume, degree of grafting and crosslinking, as well as by molecular characteristics of the PS matrix. Most HIPS grades contain 5–7% of rubber, which covers the total volume fraction from 20 to 30%. For optimum toughening, the rubber particles of several micrometers are required. For good surface appearance a bimodal particle size distribution of rubber phase (eg, 2 and 0.2 $\mu$m) is desirable. The presence of rubber phase in the PS matrix substantially improves not only impact strength but affects also other properties compared with styrene homopolymer. Thus elasticity modulus, tensile strength, and hardness somewhat decrease while elongation and melt viscosity increase. All things considered, HIPS shows balanced complex end-use properties, which is advantageous in a broad application sphere.

HIPS is currently processed by procedures such as injection molding, extrusion, blow-molding, and thermoforming. HIPS properties can be further modified by incorporation of special additives such as flame retardants, stabilizers, antistatic agents, etc. The main production fraction of HIPS is consumed in the manufacture of packaging materials, technical products, toys, and various consumer goods.

**Acrylonitrile-Butadiene-Styrene Polymer.** The name acrylonitrile–butadiene–styrene (ABS) polymer is reserved for a family of thermoplastics with the SAN matrix containing dispersed elastomer particles.The oldest approach to the ABS preparation, similarly as in the case of HIPS, is mechanical blending of individual components. At present the graft polymerization of a mixture of styrene with acrylonitrile in the presence of a suitable rubber component is the current process of ABS polymer manufacture. Most producers employ some form of emulsion technology, but the mass or mass-emulsion polymerization is also technologically feasible (60,272).

Common types of ABS have an average composition of 21–27% acrylonitrile, 12–25% butadiene, and 54–63% styrene. The styrene component contributes good processability and stiffness to the final ABS, butadiene increases the impact strength, and acrylonitrile improves chemical and heat deformation resistance. The two-phase system where rubber particles are dispersed in the matrix of SAN shows a morphology similar to HIPS, but the particle size is smaller with fewer SAN subinclusions than those in HIPS. ABS polymer shows excellent toughness combined with good thermal and chemical resistance, high elastic modulus, and good appearance.

ABS can be processed by all common molding technologies. The main consumption of this polymer is for household appliances, automotive parts, business machine and telephone components, electrical devices, pipes and fittings, and leisure-time equipment.

**Poly(2,6-dimethyl-1,4 phenylene oxide)/High Impact Polystyrene (PPO/HIPS).** Poly (phenylene oxide) is a polymer with high heat deformation resistance, excellent electrical properties, and high resistance to acids and bases. Because of high melt viscosity, PPO is blended with styrene polymers to achieve rheological properties necessary for processing by current technologies. Improvement in PPO toughness is obtained simultaneously with viscosity decrease if HIPS is used as a modifier. Rubber particles distributed uniformly throughout the new matrix are responsible for an increase in toughness, and polystyrene improves its processability. Unlimited PPO/PS miscibility enables preparation of blends of broad composition scale with well-balanced end-use properties. For high performance applications in electrotechnical and automotive industries, high impact blends of PPO with ABS, PA, or PC are manufactured.

**Polypropylene/Rubber.** Polypropylene (PP) is a versatile polymer with good resistance to heat, chemicals and solvents, and good electrical properties. Other properties can be improved by compounding with various nonpolymeric additives as well as with polymers. Blending with elastomers and copolymerizing with other monomers are used for toughening of this polymer (314,315). Synthetic elastomers as EPM, SEBS, PIB, and natural rubber are incorporated into PP matrix by mechanical blending. Especially PP/EPM blends are of considerable practical importance. These blends with a low EPM content are used as high impact polypropylene, the blends with high content of this elastomer can be used as thermoplastic elastomers. Phase structure control of modified PP depends strongly on molecular characteristics of the matrix (crystallinity, crosslinked part etc.) and therefore it is relatively difficult to achieve the desired and sufficiently stabile blend morphology. The presence of rubber particles in PP matrix increases the

impact strength, but leads to lower tensile strength, stiffness, and heat deformation resistance. The set of end-use properties is convenient mainly for application in automotive industry.

**Poly(vinylchloride)/Rubber.** PVC is an important commodity polymer with good chemical resistance and low flammability. Without modification, however, it is not practically processable, and its mechanical properties and heat resistance are very poor. Therefore, various additives as lubricants, stabilizers, and impact modifiers are incorporated to PVC grains to obtain versatile polymer.

To achieve good toughness, required for many applications, impact modifiers are added to PVC. Chlorinated polyethylenes, ethylene-vinyl acetate copolymers, styrene-methyl methacrylate grafted elastomers, vinyl rubbers, and polyacrylates are the most frequently used (316). These polymers are blended together with other additives. Blending conditions are extraordinarly important for morphology control and consequently for final properties of the blends.

Most of high impact PVC blend production is consumed in civil engineering applications. Because of low price and ability to be properly modified, this oldest commercially produced polymer remains one of the most important synthetic materials.

**Polyamide/Rubber Blends.** The family of polyamides (PA) encompasses polymers with a variety of chemical compositions. A characteristic feature of these polymers is poor toughness at low temperature and/or in the presence of notches. Multi-year efforts to improve their toughness has resulted in numerous modification procedures (317). Most are based on melt blending of acid or anhydride-containing elastomers with PA. At present, producers of toughened PA typically use rubbers containing small amount of maleic anhydride (up to 2%). During blending, reactive compatibilization takes place. The maleic-anhydride groups react with amino groups of PA giving rise to graft copolymers at the interface. Saturated rubbers, eg, EPDM, SEBS, or BR are used. The obtained morphology shows the dispersed rubber particles of size between 0.001–0.1 $\mu$m. Compatibilization based on the reaction of anhydride and amino groups is also utilized for preparation of engineering materials as PA/PP, PA/ABS, or PA/PPO blends.

**Polycarbonate Blends.** Polycarbonates (PC) are classified as construction plastics because of their high heat deformation temperature, electric properties, and mechanical characteristics including impact strength. Similarly, as in the case of polyamides, they do not achieve the required toughness if notched or if exposed to low temperature. Therefore, polycarbonates are blended with ABS polymer to combine their properties with the toughness of ABS. No compatibilizer is needed in the blending of both the components as SAN and PC are partly miscible (313).

PC/ABS blends are materials with an excellent combination of end-use properties, improved processability and, moreover, an acceptable cost. A broad scale of PC/ABS types is used in the automotive industry and other engineering applications.

**Recyclates of Polymers.** Blending of polymers is an important aspect of the recycling technologies that aim to overcome the problem of separation (sorting) mixed polymeric waste into pure feedstock streams by direct processing of mixed materials with or without compatibilizers (318,319). Mechanical recycling of commingled plastic waste may be viewed as a compromise between conflicting

requirements. That is, sorting of the waste is expensive, but can give recyclates of higher quality; on the other hand, reprocessing of commingled plastics is relatively inexpensive, but the resulting product shows lower mechanical and aesthetic properties. In any case, under certain circumstances, the mechanical blending of mixed plastics waste can be advantageous from both the economical and ecological viewpoints.

For reprocessing of mixed plastics, either current processing machines or special machinery for manufacturing large profiles are used. The recyclates, called plastic lumber, suffer from inferior mechanical performance due to immiscibility, and thus poor adhesion of components. Moreover, the presence of heterogeneities and particulate contamination restricts application of the products. Therefore, commingled plastics are often processed into large profiles which can rather fulfill requirements for strength characteristics. For manufacture of such profiles, specific procedures have been developed. Thus, the intrusion process combines extrusion of mixed plastics with melt filling to a large mold without using screenpack or an extrusion nozzle (Klobbie process) (319). Continuous extrusion produces linear profiles with large cross-sections of molten polymer materials that are then extruded into cooled dies.

For more demanding applications, the commingled plastic wastes as well as partially sorted plastics mixture can be processed using compatibilizers. Recyclates with good mechanical properties as well as appearance have been reported. Thus, a mixture of polyolefins blended with organic peroxides or with a combination of peroxides and liquid PB gives materials of the same or higher impact resistance than the virgin HDPE (57). A mixture of polyolefins and styrene plastics blended with a multicomponent compatibilizer (combination of SB and EPDM copolymers) shows excellent impact strength and acceptable mechanical properties. Still better results have been obtained with a compatibilization system containing, besides copolymers, stabilizers based on aromatic amines. This combination shows even a synergistic effect (320). It seems that in case, the mixed polymers are not seriously damaged during their life cycle the compatibilization and restabilization can be an advantageous way of material recycling.

## BIBLIOGRAPHY

"Polyblends" in *EPST* 1st ed., Suppl. Vol. 2, pp. 458–484, by R. D. Deanin, University of Lowell; "Polymer Blends" in *EPSE* 2nd ed., Vol. 12, pp. 399–461, by D. P. Paul, J. W. Barlow, and H. Keskkula, University of Texas.

1. L. A. Utracki, *Polymer Alloys and Blends, Thermodynamic and Rheology*, Hanser Publishers, Munich, 1989.
2. J. W. Gibbs, *Trans. Conn. Acad. Sci.* **3**, 228 (1976).
3. G. L. Lewis and M. Randall, *Thermodynamics*, McGraw-Hill, New York, 1961.
4. P. J. Flory, *Principles of Polymer Chemistry*, Cornell University Press, Ithaca, N.Y., 1953.
5. O. Olabisi, L. Robeson, and M. T. Shaw, *Polymer—Polymer Miscibility*, Academic Press, Inc., New York, 1979.
6. D. R. Paul and S. Newman, eds., *Polymer Blends*, Vols. I, II, Academic Press, Inc., New York, 1978.

7. D. R. Paul, J. W. Barlow, and H. Keskula, in J. I. Kroschwitz, ed.-in-ch, *Encyclopedia of Polymer Science and Engineering* 2nd ed., Wiley-Interscience, New York, 1985.
8. P. J. Flory, *J. Am. Chem. Soc.* **86**, 1833 (1965).
9. L. P. McMaster, *Macromolecules* **6**, 760 (1973).
10. P. J. Flory, R. A. Orwoll, and A. Vrij, *J. Am. Chem. Soc.* **86**, 3515 (1964).
11. B. E. Eichinger and P. J. Flory, *Trans. Faraday Soc.* **64**, 2035 (1968).
12. D. Patterson, *Macromolecules* **2**, 672 (1969).
13. D. Patterson and A. Robard, *Macromolecules* **11**, 690 (1978).
14. I. C. Sanchez and R. H. Lacombe, *J. Phys. Chem.* **80**, 2352 (1976).
15. I. C. Sanchez, *Polym. Eng. Sci.* **24**, 79 (1984).
16. Yu. S. Lipatov and A. E. Nesterov, *Thermodynamics of Polymer Blends*, Technomic Publishing Co., Lancaster, Pa., 1997, Chap. 5, pp. 275–361.
17. Coleman, J. F. Graf, and P. C. Painter, *Specific Interactions and the Miscibility of Polymer Blends*, Technomic Publishing Co., Lancaster, Pa., 1991.
18. R. Koningsveld, W. H. Stockmayer, and E. Nies, *Polymer Phase Diagrams*, Oxford University Press, Oxford, U.K. 2001.
19. H. J. Jeon, J. H. Lee, and N. P. Balsara, *Macromolecules* **31**, 3328 (1998).
20. S. Zhu and D. R. Paul, *Polymer* **44**, 5671 (2003).
21. J. W. Cahn, *Trans. Metall. Soc., AIME* **242**, 166 (1968).
22. E. Roerdink and G. Challa, *Polymer* **21**, 1161 (1980).
23. J. W. Schurer, A. deBoer, and G. Challa, *Polymer* **16**, 201 (1975).
24. I. C. Sanchez, *Physics of Polymer Surfaces and Interfaces*, Butterworth-Heiemann, Boston, Mass., 1992.
25. S. Wu, *Polymer Interface and Adhesion*, Dekker, Inc., New York, 1982.
26. L. Leibler, *Makromol. Chem., Macromol. Symp.* **16**, 1 (1988).
27. D. Broseta, G. H. Fredrickson, E. Helfand, and L. Leibler, *Macromolecules* **23**, 132 (1990).
28. L. Leibler, H. Orland, and J. C. Wheeler, *J. Chem. Phys.* **79**, 3550 (1983).
29. D. Mathur, R. Hariharan, and E. B. Neuman, *Polymer* **40**, 6077 (1999).
30. S. B. Chun and C. D. Han, *Macromolecules* **32**, 4030 (1999).
31. R. B. Thompson and M. W. Matsen, *J. Chem. Phys.* **112**, 6863 (2000).
32. J. R. Kim, A. M. Jamieson, S. D. Hudson, I. Manas-Zloczower, and H. Ishida, *Macromolecules* **31**, 5383 (1998).
33. A. Adedeji, S. D. Hudson, and A. I. Jamieson, *Polymer* **38**, 737 (1997).
34. D. Gersappe, P. K. Horn, D. Irvine, and A. C. Balazs, *Macromolecules* **27**, 720 (1994).
35. E. A. Eastwood and M. D. Dadmun, *Macromolecules* **35**, 5069 (2002).
36. M. D. Dadmun, *Macromolecules* **33**, 9122 (2000).
37. B. D. Edgecombe, J. A. Stein, J. M. J. Frechet, Z. Xu, and E. J. Kramer, *Macromolecules* **31**, 1292 (1998).
38. J. Li and D. Favis, *Polymer* **43**, 4935 (2002).
39. N. Marin and D. Favis, *Polymer* **43**, 4723 (2002).
40. L. Leibler, *Makromol. Chem., Rapid Commun.* **2**, 393 (1981).
41. H. S. Jeon, J. H. Lee, and N. P. Balsara, *Macromolecules* **31**, 3328 (1998).
42. H. S. Jeon, J. H. Lee, N. P. Balsara, and N. C. Newstein, *Macromolecules* **31**, 3340 (1998).
43. J. H. Lee, N. P. Balsara, A. K. Chakraborty, R. Krishnamorti, and B. Hammouda, *Macromolecules* **35**, 7748 (2002).
44. L. Corte, K. Yamauchi, F. Court, M. Cloitre, T. Hashimoto, and L. Leibler, *Macromolecules* **36**, 7695 (2003).
45. S. Datta and D. J. Lohse, *Polymeric Compatibilizers*, Carl Hanser Verlag, Munich 1996, pp. 41–59.

46. W. E. Baker, C. Scott, and G. H. Hu, eds., *Reactive Polymer Blending*, Carl Hanser Verlag, Munich, 2001.
47. M. J. Folkes and P. S. Hope, eds., *Polymer Blends and Alloys*, Chapman & Hall, London, 1993.
48. D. R. Paul and C. B. Bucknall, eds., *Polymer Blends*, John Wiley & Sons, New York, 2000, pp. 539–579.
49. R. Fayt, R. Jerome, and Ph. Teyssie, *J. Polym. Sci., Polym. Phys.* **20**, 2209 (1982).
50. R. Fayt, R. Jerome, and Ph. Teyssie, *Polym. Eng. Sci.* **27**, 328 (1987).
51. R. Fayt, R. Jerome, and Ph. Teyssie, *J. Polym. Sci., Polym. Phys.* **27**, 775 (1989).
52. R. Fayt, R. Jerome, and Ph. Teyssie, *Polym. Eng. Sci.* **30**, 937 (1990).
53. G. P. Hellmann and M. Dietz, *Macromol. Symp*. **170**, 1 (2001).
54. C. Creton, E. J. Kramer, H. R. Brown, and C. Y. Hui, *Adv. Polym. Sci.* **156**, 53 (2002).
55. S. Al Malaika, ed., *Reactive Modifiers for Polymers*, Chapman & Hall, London, 1997, pp. 84–159.
56. W. E. Baker, C. Scott, and G. H. Hu, eds., *Reactive Polymer Blending*, Carl Hanser Verlag, Munich, 2001, pp. 255–280.
57. Z. Kruliš, Z. Horák, F. Lednický, J. Pospíšil, and M. Sufčák, *Angew. Makromol. Chem.* **258**, 63 (1998).
58. H. X. Zhang and D. J. Hourston, *J. Appl. Polym. Sci*. **71**, 2049 (1999).
59. J. Schies and D. B. Priddy eds., *Modern Styrenic Polymers: Polystyrene and Styrenic Copolymers*, John Wiley & Sons, Chichester, U.K., 2003.
60. B. D. Gesner, *Encyclopedia of Polymer Science and Technology*, Vol. 10, Interscience, New York, 1969, pp. 694–709.
61. R. D. Deanin, in H. F. Mark, N. G. Gaylord, and N. M. Bikales, eds., *Encyclopedia of Polymer Science and Technology*, Suppl. Vol. 2, Wiley-Interscience, New York, 1977, p. 458.
62. A. P. Smith, H. Ade, S. D. Smith, C. C. Koch, and R. J. Spartac, *Macromolecules* **34**, 1536 (2001); N. Furgiuele, A. H. Lebowitz, K. Khait, and J. M. Torkelson, *Polym. Eng. Sci.* **40**, 1447 (2000).
63. L. H. Sperling, *Interpenetrating Polymer Networks and Related Materials*, Plenum Press, New York, 1981.
64. C. E. Scott and C. W. Macosko, *Polym. Bull.* **26**, 341 (1991).
65. C. E. Scott and C. W. Macosko, *Polymer* **36**, 461 (1995).
66. U. Sundararaj, C. W. Macosko, A. Nakayama, and T. Inoue, *Polym. Eng. Sci.* **35**, 100 (1995).
67. U. Sundararaj, C. W. Macosko, and Chi-Kai Shih, *Polym. Eng. Sci.* **36**, 1769 (1996).
68. C. W. Macosko, *Macromol. Symp.* **149**, 171 (2000).
69. P. Pötschke and D. R. Paul, *J. Macromol. Sci.* **C43**, 87 (2003).
70. B. D. Favis, in D. R. Paul and C. B. Bucknall, eds., *Polymer Blends Vol. 1: Formulations*, John Wiley & Sons, Inc., New York, 2000, Chap. 16.
71. D. R. Paul and J. W. Barlow, *J. Macromol. Sci., Rev. Macromol. Chem.* **C18**, 108 (1980).
72. S. Miles and A. Zurek, *Polym. Eng. Sci.* **28**, 796 (1988).
73. V. I. Metelkin and V. P. Blekht, *Colloid J. USSR* **46**, 425 (1984).
74. V. Everaert, L. Aerts, and G. Groeninckx, *Polymer* **40**, 6627 (1999).
75. H. Van Oene, in D. R. Paul and S. Newman, eds., *Polymer Blends*, Vol. 2, Academic Press, Inc., New York, 1978, p. 295.
76. D. Bourry and B. D. Favis, *J. Polym. Sci., Part B: Polym. Phys.* **36**, 1889 (1998).
77. S. Steinmann, W. Gronski, and C. Friedrich, *Rheol. Acta* **41**, 77 (2002).
78. J. Lyngaae-Jørgensen and L. A. Utracki, *Makromol. Chem., Macromol. Symp.* **48/49**, 189 (1991).
79. R. Willemse, A. Posthuma de Boer, J. van Dam, and A. D. Gotsis, *Polymer* **39**, 5879 (1998).

80. J. K. Lee and C. D. Han, *Polymer* **40**, 6277 (1999).
81. C. Z. Chuai, K. Almdal, and J. Lyngaae-Jørgensen, *Polymer* **44**, 481 (2003).
82. B. D. Favis, C. Lavalle, and A. Derdouri, *J. Mater. Sci.* **27**, 4211 (1992).
83. S. Y. Hobbs, M. E. J. Dekkers, and W. H. Watkins, *J. Mater. Sci.* **23**, 1598 (1988).
84. H. F. Guo, S. Packirisamy, N. V. Gvozdic, and D. J. Meier, *Polymer* **38**, 785 (1997).
85. I. Luzinov, C. Pagnoulle, and R. Jérôme, *Polymer* **41**, 7099 (2000).
86. N. Henmati, H. Nazokdast, and H. S. Panahi, *J. Appl. Polym. Sci.* **82**, 1129 (2001).
87. N. Nemirovski, A. Siegmann, and M. Narkis, *J. Macromol. Sci., Phys.* **B34**, 459 (1995).
88. A. K. Gupta and K. R. Shrinivasan, *J. Appl. Polym. Sci.* **47**, 167 (1993).
89. J. Reignier, B. D. Favis, and M.-C. Heuzey, *Polymer* **44**, 49 (2003).
90. J. Lyngaae-Jørgensen, in M. J. Folkes and P. S. Hope, eds., *Polymer Blends and Alloys*, Blackie Academic & Professional, London, 1993, Chap. 4.
91. J. M. H. Janssen, in H. E. H. Meijer, ed., *Materials Science and Technology, Vol. 8: Processing of Polymers*, Wiley-VCH, Weinheim, 1997, Chap. 3.
92. H. E. H. Meijer and J. M. H. Janssen, in I. Manas-Zloczower and Z. Tadmor, eds., *Mixing and Compounding of Polymers*, Hanser Publishers, Munich, 1994, Chap. 4.
93. L. A. Utracki and Z. H. Shi, *Polym. Eng. Sci.* **32**, 1824 (1992).
94. I. Fortelný, J. Kovář, and M. Stephan, *J. Elastomers Plast.* **28**, 106 (1996).
95. H. A. Stone, *Annu. Rev. Fluid Mech.* **26**, 65 (1994).
96. C. L. Tucker and P. Moldenaers, *Annu. Rev. Fluid Mech.* **34**, 177 (2002).
97. J. M. H. Janssen and H. E. H. Meijer, *J. Rheol.* **37**, 597 (1993).
98. J. T. Overbeek, in H. K. Kruyt, ed., *Kinetic of Flocculation, Colloid Science* Vol. 1, Elsevier, Amsterdam, The Netherlands, 1952, p. 278.
99. J. J. Elmendorp, in C. Rauwendaal, ed., *Mixing in Polymer Processing*, Marcel Dekker, Inc., New York, 1991, p. 17.
100. I. Fortelný, *Macromol. Symp.* **158**, 137 (2000).
101. S. T. Milner, H. Xi, *J. Rheol.* **40**, 663 (1996).
102. A. K. Chesters, *Trans. I. Chem. E.* **69A**, 259 (1991).
103. H. Wang, A. Z. Zinchenko, and R. H. Davis, *J. Fluid Mech.* **265**, 161 (1994).
104. M. A. Rother and R. H. Davis, *Phys. Fluids* **13**, 1178 (2001).
105. I. Fortelný and A. Živný, *Rheol. Acta* **42**, 454 (2003).
106. N. Tokita, *Rubber Chem. Technol.* **50**, 292 (1977).
107. J. J. Elmendorp and A. K. Van der Vegt, *Polym. Eng. Sci.* **26**, 1332 (1986).
108. I. Fortelný and J. Kovář, *Eur. Polym. J.* **25**, 317 (1988).
109. J. Lyngaae-Jørgensen and A. Valenza, *Makromol. Chem., Macromol. Symp.* **38**, 43 (1990).
110. I. Fortelný and A. Živný, *Polym. Eng. Sci.* **35**, 1872 (1995).
111. M. Huneault, Z. H. Shi, and L. A. Utracki, *Polym. Eng. Sci.* **35**, 115 (1995).
112. J. M. H. Janssen and H. E. H. Meijer, *Polym. Eng. Sci.* **35**, 1766 (1995).
113. L. Delamare, B. Vergnes, *Polym. Eng. Sci.* **36**, 1685 (1996).
114. S. A. Patlazhan and J. T. Lindt, *J. Rheol.* **40**, 1095 (1996).
115. H. Potente and M. Bastian, *Polym. Eng. Sci.* **40**, 727 (2000).
116. I. Fortelný, *Rheol. Acta* **40**, 485 (2001).
117. P. Van Puyvelde, H. Yang, J. Mewis, and P. Moldenaers, *J. Rheol.* **44**, 1401 (2000).
118. B. D. Favis and J. M. Willis, *J. Polym. Sci., Part B: Polym. Phys.* **28**, 2259 (1990).
119. I. Fortelný, D. Kamenická, and J. Kovář, *Angew. Makromol. Chem.* **164**, 125 (1988).
120. P. G. Ghondgaonkar and U. Sundararaj, *Polym. Eng. Sci.* **36**, 1656 (1996).
121. W. Lerdwijitjarud, A. Sirivat, and R. G. Larson, *Polym. Eng. Sci.* **42**, 798 (2002).
122. Z. H. Shi and L. A. Utracki, *Polym. Eng. Sci.* **32**, 1834 (1992).
123. I. Fortelný, D. Michálková, and J. Mikešová, *J. Appl. Polym. Sci.* **59**, 155 (1996).
124. N. Grizzuti and O. Bifulco, *Rheol. Acta* **36**, 406 (1997).
125. A. P. Plochocki, S. S. Dagli and R. D. Andrews, *Polym. Eng. Sci.* **30**, 741 (1990).

126. I. Fortelný, Z. Černá, J. Binko, and J. Kovář, *J. Appl. Polym. Sci.* **48**, 1731 (1993).
127. B. D. Favis and J. P. Chalifoux, *Polym. Eng. Sci.* **27**, 1591 (1987).
128. B. D. Favis, *J. Appl. Polym. Sci.* **39**, 285 (1990).
129. O. Franzheim, T. Rische, M. Stephan, and W. J. MacKnight, *Polym. Eng. Sci.* **40**, 1143 (2000).
130. H. Potente, S. Krawinkel, M. Bastian, M. Stephan, and P. Pötschke, *J. Appl. Polym. Sci*. **82**, 1986 (2001).
131. I. Fortelný, D. Michálková, J. Koplíková, E. Navrátilová, and J. Kovář, *Angew. Makromol. Chem.* **179**, 185 (1990).
132. I. Fortelný, R. Rosenberg, and J. Kovář, *Polym. Networks Blends* **3**, 35 (1993).
133. M. A. Huneault, F. Mighri, G. H. Ko, and F. Watanabe, *Polym. Eng. Sci*. **41**, 672 (2001).
134. H. A. Stone, B. J. Bentley, and L. G. Leal, *J. Fluid Mech.* **173**, 131 (1989).
135. H. A. Stone and L. G. Leal, *J. Fluid Mech.* **198**, 399 (1989).
136. R. C. Willemse, R. J. J. Ramaker, J. Van Dam, and A. Posthuma de Boer, *Polym. Eng. Sci.* **39**, 1717 (1999).
137. H. Veenstra, J. Van Dam, and A. Posthuma de Boer, *Polymer* **41**, 3037 (2000).
138. I. Fortelný, A. Živný, and J. Jza, *J. Polym. Sci., Part B: Polym. Phys.* **37**, 181 (1999).
139. I. Fortelný and A. Živný, *Polymer* **39**, 2669 (1998).
140. F. M. Mirabella, *J. Polym. Sci., Polym. Phys. Ed.* **32**, 1205 (1995).
141. B. Crist and A. R. Nesarikar, *Macromolecules* **28**, 890 (1995).
142. W. R. White and P. Wiltzius, *Phys. Rev. Lett.* **75**, 3012 (1995).
143. K. Wallheinke, P. Pötschke, C. W. Macosko, and H. Stutz, *Polym. Eng. Sci.* **39**, 1022 (1999).
144. J. Lyngaae-Jørgensen, K. Lunde Rasmussen, E. A. Chtcherbakova, and L. A. Utracki, *Polym. Eng. Sci.* **39**, 1060 (1996).
145. D. Boury and B. D. Favis, *J. Polym. Sci., Part B: Polym. Phys.* **36**, 1889 (1998).
146. P. T. Hijetaoja, R. M. Holsti-Miettinen, J.V. Sepälä, and O. T. Ikkala, *J. Appl. Polym. Sci.* **54**, 1613 (1994).
147. I. Fortelný, D. Michálková, J. Hromádková, and F. Lednický, *J. Appl. Polym. Sci.* **81**, 570 (2001).
148. R. Fayt and P. Teyssié, *Polym. Eng. Sci.* **30**, 937 (1990).
149. P. Van Puyvelde, S. Velankar, and P. Moldenaers, *Curr. Opin. Colloid Interface Sci.* **6**, 457 (2001).
150. I. Fortelný, *J. Macromol. Sci.-Phys.* **B39**, 67 (2000).
151. J. F. Palierne and F. Lequeux, *J. Non-Newtonian Fluid Mech.* **40**, 289 (1991).
152. Su Ping Lyu, T. D. Jones, F. S. Bates, and C. W. Macosko, *Macromolecules* **35**, 7845 (2002).
153. I. Fortelný and A. Živný, *Polymer* **41**, 6865 (2000).
154. G. Xu and S. Lim, *Polymer* **37**, 421 (1996).
155. M. Taha and J. Frerejean, *J. Appl. Polym. Sci.* **61**, 969 (1996).
156. M. Wagner and B. A. Wolf, *Polymer* **34**, 1460 (1993).
157. T. Appleby, F. Czer, G. Moad, E. Rizzardo, and C. Stavropulos, *Polym. Bull.* **32**, 479 (1994).
158. Z. Horák, V. Fořt, D. Hlavatá, F. Lednický, and F. Večerka, *Polymer* **37**, 66 (1996).
159. T. Li, V. A. Topolkaraev, A. Hiltner, E. Baer, X. Y. Ji, and R. P. Quirk, *J. Polym. Sci., Part B: Polym. Phys.* **33**, 667 (1995).
160. E. Kroeze, G. ten Brinke, and G. Hadziioannou, *Polym. Bull. (Berlin)* **38**, 210, (1997).
161. D. Hlavatá, Z. Horák, F. Lednický, and Z. Tuzar, *Polym. Networks Blends* **7**, 195 (1997).
162. D. Hlavatá, Z. Horák, J. Hromádková, F. Lednický, and A. Pleska *J. Polym. Sci., Part B: Polym. Phys.* **37**, 1647 (1999).
163. J. Noolandi, *J. Macromol. Chem. Theory Simul.* **1**, 295 (1992).

164. G. Gersappe, P. K. Harm, D. Irvine, and A. C. Balazs, *Macromolecules* **27**, 720 (1994).
165. H. Feng, J. Tian, and C. Ye, *J. Appl. Polym. Sci.* **61**, 2265 (1996).
166. T. J. Cavanaugh, K. Buttle, J. N. Turner, and E. B. Nauman, *Polymer* **39**, 4191 (1998).
167. Z. Horák, D. Hlavatá, J. Hromádková, J. Kotek, V. Hašová, J. Mikešová, and A. Pleska, *J. Polym. Sci., Part B: Polym. Phys.* **40**, 2612 (2002).
168. D. Hlavatá, J. Hromádková, I. Fortelný, V. Hašová, and J. Pulda, *J. Appl. Polym. Sci.* **92**, 2431( 2004).
169. K. H. Dai, J. Washiyama, and E. J. Kramer, *Macromolecules* **27**, 4544 (1994).
170. D. Hlavatá, Z. Horák, F. Lednický, J. Hromádková, A. Pleska, and V. Zanevskii, *J. Polym. Sci., Part B: Polym. Phys.* **39**, 931 (2001).
171. I. Fortelný, D. Hlavatá, J. Mikešová, D. Michálková, L. Potroková, and I. Šloufová, *J. Polym. Sci., Part B: Polym. Phys.* **41**, 609 (2003).
172. I. Fortelný, J. Mikešová, J. Hromádková, V. Hašová, and Z. Horák, *J. Appl. Polym. Sci.* **90**, 2303 (2003).
173. Z. Horák, D. Hlavatá, I. Fortelný, and F. Lednický, *Polym. Eng. Sci.* **42**, 2042 (2002).
174. S. Wu, *Polym. Eng. Sci.* **30**, 753 (1990).
175. T. A. Kavassalis and J. Noolandi, *Macromolecules* **22**, 2709 (1989).
176. J. W. Barlow and D. R. Paul, *Polym. Eng. Sci.* **24**, 525 (1984).
177. S. C. Tjong and S. A. Xu, *J. Appl. Polym. Sci.*, **68**, 1099 (1998).
178. P. Cigana, B. D. Favis, C. Albert, and T. Vu-Khanh, *Macromolecules* **30**, 4163 (1997).
179. G. Radonjič, V. Musil, and I. Šmit, *J. Appl. Polym. Sci.* **69**, 2625 (1998).
180. I. Šmit and G. Radonjič, *Polym. Eng. Sci.* **40**, 2144 (2000).
181. C. Harrats, R. Fayt, and R. Jerome, *Polymer* **43**, 863 (2002).
182. L. E. Alexander, *X-Ray Diffraction Methods in Polymer Science*. Wiley-Interscience, New York, 1969.
183. C. Sadron and B. Galott, *Makromol. Chem.* **164**, 301 (1973).
184. F. S. Bates, R. E. Cohen, and C. V. Berney, *Macromolecules* **15**, 589 (1982).
185. F. J. Balta-Calleja and C. G. Vonk, *X-ray Scattering of Synthetic Polymers*. Elsevier, Amsterdam, The Netherlands, 1989.
186. L. Leibler, *Makromol. Chem., Macromol. Symp.* **16**, 1 (1988).
187. D. Mathur, R. Hariharan, and E. B. Nauman, *Polymer* **40**, 6077 (1999).
188. R. S. Stein, in D. R. Paul, and S. Newman, eds., *Polymer Blends*, Vols. I and II, Academic Press, Inc., New York, 1978, Chapt. 9.
189. R. J. Composto, J. W. Mayer, E. J. Kramer, and D. M. White, *Phys. Rev. Lett.* **57**, 1312 (1986).
190. G. D. Wignall and J. I. Kroschwitz, eds., *Encyclopedia of Polymer Science and Engineering*, Vol. 10, Wiley-Interscience, New York, 1987, p. 112.
191. M. M. Agamalian, R. G. Alamo, J. D. Londono, L. Mandelkern, and G. D. Wignall, *J. Appl. Cryst.* **33**(1), 843 (2000).
192. M. T. Shaw, in D. J. Walsh, J. S. Higgins, and A. Maconnachie, eds., NATO Series E No. 89, Martinns Nijhoff Publishers, Dordrecht, The Netherlands, 1985.
193. B. Brahimi, A. Ait-Kadi, A. Ajji, and R. Fayt, *J. Polym. Sci., Part B: Polym. Phys.* **29**, 945 (1991).
194. I. Fortelný and D. Michálková, *Plast., Rubber Compos. Process. Appl.* **27**(2), 53 (1998).
195. K. Kato, *J. Electron Microsc. Jpn.* **14**, 219 (1965).
196. J. S. Trent, J. I. Scheinbeim, and P. R. Couchman, *Macromolecules* **16**, 589 (1983).
197. G. Radonjič, *J. Appl. Polym. Sci.* **72**, 291 (1999).
198. Chi-An Dai, K. D. Jandt, D. R. Iyengar, N. L. Slack, K. H. Dai, W. B. Davidson, E. J. Kramer, and Chung-Yuen Hui, *Macromolecules* **30**, 549 (1997).
199. K. Sondergaard and J. Lyngaae-Jorgensen, *Rheo-Physics of Multiphase Polymer Systems*, Tecnomic, Lancaster, Pa., 1995.

200. G. Schlatter, C. Serra, M. Bouquey, R. Muller, and J. Terrisse, *Polym. Eng. Sci.* **42**(10), 1965 (2002).
201. Y. A. Akpalu and Y. Y. Lin, *J. Polym. Sci., Part B: Polym. Phys.* **40**, 2714 (2002).
202. W. J. Macknight, F. E. Karasz, and J. R. Fried, in *Polymer Blends*, D. R. Paul and S. Newman, eds., Academic Press, Inc., New York, 1978, Chap. 5.
203. J. Baldrian, M. Steinhart, P. Vlček, M. Horký, P. Laggner, H. Amenitsch, and S. Bernstorff, *J. Macromol. Sci., Part B-Physics* **41**, 1023 (2002).
204. H. Amenitsch, S. Bernstorff, M. Kriechbaum, D. Lombardo, H. Mio, M. Rappolt, and P. J. Lagner, *Appl. Crystallogr.* **30**, 872 (1997).
205. I. Campoy, M. A. Gomez, and C. Marco, *Polymer* **40**, 4259 (1999).
206. A. R. Hopkins, P. G. Rasmussen, R. A. Basheer, B. K. Annis, and G. D. Wignall, *Synth. Met.* **95**, 179 (1998).
207. G. D. Wignall, R. G. Alamo, J. D. Londono, L. Mandelkern, M. H. Kim, J. S. Lin, and G. M. Brown, *Macromolecules* **33**, 551 (2000).
208. D. J. Kinning, E. L. Thomas, and L. J. Fetters, *J. Chem. Phys.* **90**, 15 (1989).
209. J. Furukawa, *Physical Chemistry of Polymer Rheology*, Springer-Verlag, Berlin, 2003, p. 217.
210. J. Lyngaae-Jorgensen, K. Lunde Rasmuseen, E. A. Chtcherbakova, and L. A. Utracki, *Polym. Eng. Sci.* **39**, 1060 (1999).
211. J. Kolařík, *Polym. Compos.* **18**, 433 (1997).
212. J. Lyngaae-Jorgensen, A. Kuta, K. Sondergaard, and K. V. Poulsen, *Polym. Networks Blends* **3**, 1 (1993).
213. J. Lyngaae-Jorgensen and L. A. Utracki, *Polymer* **44**, 1661 (2003).
214. R. C. Willemse, A. Posthuma de Boer, J. van Dam, and A. D. Gotsis, *Polymer* **40**, 827 (1999).
215. H. Veenstra, J. van Dam, and A. Posthuma de Boer, *Polymer* **40**, 1119 (1999).
216. L. E. Nielsen, *Predicting the Properties of Mixtures: Mixture Rules in Science and Engineering*, Marcel Dekker, Inc., New York, 1978, p. 51.
217. L. E. Nielsen and R. F. Landel, *Mechanical Properties of Polymers and Composites*, Marcel Dekker, Inc., New York, 1994, p. 384.
218. S. McGee and R. L. McCullough, *Polym. Compos.* **2**, 149 (1981).
219. J. Kolařík, G. L. Agrawal, Z. Kruliš, and J. Kovář, *Polym. Compos.* **7**, 463 (1986).
220. J. Kolařík, J. Velek, G. L. Agrawal, and I. Fortelný, *Polym. Compos.* **7**, 472 (1986).
221. J. Kolařík, *Polym. Networks Blends* **5**, 87 (1995).
222. J. Kolařík, *Polym. Eng. Sci.* **36**, 2518 (1996).
223. J. Kolařík, *Eur. Polym. J.* **34**, 585 (1998).
224. P.G. De Gennes, *J. Phys., Lett. (Paris)* **37**, L1 (1976).
225. J. Sax and J. M. Ottino, *Polym. Eng. Sci.* **23**, 165 (1983).
226. W. Y. Hsu and S. Wu, *Polym. Eng. Sci.* **33**, 293 (1993).
227. H. Matsuyama, M. Teramoto, and M. Tsuchyia, *J. Membr. Sci.* **118**, 177 (1996).
228. N. Marin, B. D. Favis, *Polymer* **43**, 4723 (2002).
229. J. Kolařík, *Polym. Eng. Sci.* **36**, 2518 (1996).
230. J. Kolařík and G. Geuskens, *Polym. Networks Blends* **7**, 13 (1997).
231. D. E. Kirkpatrick, J. K. McLemore, and M. A. Wright, *J. Appl. Polym. Sci.* **46**, 377 (1992).
232. R. M. Christensen, *Mechanics of Composite Materials*, John Wiley & Sons, Inc., New York, 1979.
233. J. Kolařík, J. Janáček, and L. Nicolais, *J. Appl. Polym. Sci.* **20**, 841 (1976).
234. J. Kolařík, A. Pegoretti, L. Fambri, and A. Penati, *J. Polym. Res.* **7**, 7 (2000).
235. D. Colombini and F. H. J. Maurer, *Macromolecules* **35**, 5891 (2002).
236. J. A. Faucher, *J. Polym. Sci., Part B: Polym. Phys.* **12**, 2153 (1974).

237. J. Kolařík, L. Fambri, A. Pegoretti, A. Penati, and P. Goberti, *Polym. Eng. Sci* **42**, 161 (2002).
238. J. Kolařík, A. Pegoretti, L. Fambri, and A. Penati, *J. Appl. Polym. Sci.* **88**, 641 (2003).
239. J. Kolařík, A. Pegoretti, L. Fambri, and A. Penati, *Macromol. Mater. Eng.* **288**, 629 (2003).
240. J. Kolařík, *J. Polym. Sci., Part B: Polym. Phys.* **41**, 736 (2003).
241. R. W. Garbella, J. Wachter, and J. H. Wendorff, *Prog. Colloid Polym. Sci.* **71**, 164 (1987).
242. J. Kolařík, F. Lednický, G. C. Locati, and L. Fambri, *Polym. Eng. Sci* **37**, 128 (1997).
243. L. Buki, E. Gonczy, E. Fekete, G. P. Hellmann, and B. Pukanszky, *Macromol. Symp.* **170**, 9 (2001).
244. J. Jančář, A. DiAnselmo, and A. T. DiBenedetto, *Polym. Eng. Sci* **32**, 1394 (1992).
245. L. Nicolais and M. Narkis, *Polym. Eng. Sci.* **10**, 97 (1971).
246. Z. Horák, J. Kolařík, M. Šípek, V. Hynek, and F. Večerka, *J. Appl. Polym. Sci.* **69**, 2615 (1998).
247. J. Kolařík, L. Fambri, A. Pegoretti, and A. Penati, *Polym. Adv. Technol.* **11**, 75 (2000).
248. J. Kolařík, *Polymer* **37**, 887 (1996).
249. L. Matějka, O. Dukh, and J. Kolařík, *Polymer* **41**, 1449 (2000).
250. J. Kolařík, G. C. Locati, L. Fambri, and A. Penati, *Polym. Networks Blends* **7**, 103 (1997).
251. J. Kolařík, *J. Macromol. Sci. Phys. B* **39**, 53 (2000).
252. J. Kolařík and L. Fambri, *Macromol. Mater. Eng.* **283**, 41 (2000).
253. C. B. Bucknall, *Toughened Plastics*, Applied Science Publisher, London, 1977, p. 243.
254. L. H. Sperling, *Polymeric Multicomponent Materials*, John Wiley & Sons, Inc., New York, 1997, p. 223.
255. Y.-W. Mai, S.-C. Wong, and X.-H. Chen, in D. R. Paul and C. B. Buckmall, eds., *Polymer Blends*, John Wiley & Sons, Inc., New York, 1999, p. 17.
256. C. B. Bucknall, in D. R. Paul, and C. B. Bucknall, eds., *Polymer Blends*, John Wiley & Sons, Inc., New York, 1999, p. 83.
257. W. Grellmann and S. Seidler, *J. Polym. Eng.* **11**, 71 (1992).
258. S. Seidler and W. Grellman, *Polym. Test.* **14**, 453 (1995).
259. A. F. Yee, *Encyclopedia of Polymer Science and Engineering* Vol. 8, Wiley-Interscience, New York, 1986, p. 36.
260. W. G. Perkins, *Polym. Eng. Sci.* **39**, 2445 (1999).
261. M. C. M. van der Sanden, in R. W. Cahn, P. Haasen, and E. J. Kramer, eds., *Materials Science and Technology*, Wiley-VCH, Weinheim, 1997, p. 579.
262. E. J. Kramer, *Adv. Polym. Sci.* **52/53**, 1 (1983).
263. E. J. Kramer, *Plast. Rubber Compos. Process. Appl.* **26**, 241 (1997).
264. G. M. Swallowe, in G. M. Swallowe, ed., *Mechanical Properties and Testing of Polymers*, Kluwer Academic Publishers, Dordrecht, 1999, p. 40.
265. S. Wu, *Polym. Eng. Sci.* **30**, 753 (1990).
266. S. Wu, *J. Appl. Polym. Sci.* **35**, 549 (1988).
267. R. J. Gaymans, in D. R. Paul, and C. B. Buckmall, eds., *Polymer Blends*, John Wiley & Sons, Inc., New York, 1999, p. 177.
268. K. Friedrich, *Adv. Polym. Sci.* **52/53**, 225 (1983).
269. C. B. Bucknall, in D. R. Paul, and C. B. Bucknall, eds., *Polymer Blends*, John Wiley & Sons, Inc., New York, 1999, p. 59.
270. A. Lazzeri and C. B. Bucknall, *J. Mater. Sci.* **28**, 6799 (1993).
271. A. S. Argon, R. E. Cohen, O. S. Gebizlioglu, and C. E. Schwier, *Adv. Polym. Sci.* **52/53**, 275 (1983).

272. P. Švec, L. Rosík, Z. Horák, and F. Večerka, *Styrene-Based Plastics and Their Modifications*, E. Horwood, London, 1990, p. 109.
273. W. Döll, *Adv. Polym. Sci.* **52/53**, 105 (1983).
274. A. Arostegui and J. Nazabal, *Polymer* **44**, 239 (2003).
275. J. Z. Liang and R. K. Y. Li, *J. Appl. Polym. Sci.* **77**, 409 (2000).
276. M. Raab, J. Kotek, J. Baldrian, and W. Grellmann, *J. Appl. Polym. Sci.* **69**, 2255 (1998).
277. J. Kotek, M. Raab, J. Baldrian, and W. Grellmann, *J. Appl. Polym. Sci.* **85**, 1174 (2002).
278. C. A. Cruz-Ramos, in D. R. Paul and C. B. Buckmall, eds., *Polymer Blends*, John Wiley & Sons, Inc., New York, 1999, p. 137.
279. P. Galli, *J. Macromol. Sci., Pure Appl. Chem. A* **36**, 1561 (1999).
280. W. Jiang, S. C. Tjong, and R. K. Y. Li, *Polymer* **41**, 3479 (2000).
281. W. Jiang, L. An, and B. Jiang, *Polymer* **42**, 4777 (2001).
282. Z. H. Liu, X. D. Zhang, X. G. Zhu, Z. N. Qi, and F. S. Wang, *Polymer* **38**, 5267 (1997).
283. T. Kurauchi and T. Ohta, *J. Mater. Sci.* **19**, 1699 (1984).
284. M. Lu, H. Keskkula, and D. R. Paul, *Polymer* **34**, 1874 (1993).
285. K. Matsushige, S. V. Radcliffe, and E. Baer, *J. Appl. Polym. Sci.* **20**, 1853 (1976).
286. I. Kelnar, M. Stephan, L. Jakisch, and I. Fortelný, *J. Appl. Polym. Sci.* **74**, 1404 (1999).
287. I. Kelnar, J. Kotek, B. S. Munteanu, and I. Fortelný, *J. Appl. Polym. Sci.* **89**, 3647 (2003).
288. Z. Bartczak, A. S. Argon, R. E. Cohen, and M. Weinberg, *Polymer* **40**, 2347 (1999).
289. W. C. J. Zuiderduin, C. Westzaan, J. Hueting, and R. J. Gaymans, *Polymer* **44**, 261 (2003).
290. M. W. L. Wilbrink, A. S. Argon, R. E. Cohen, and M. Weinberg, *Polymer* **42**, 10155 (2001).
291. C. D. Han, *Multiphase Flow in Polymer Processing*, Academic Press, Inc., New York, 1981.
292. L. A. Utracki, *Polymer Alloys and Blends*, Carl Hanser-Verlag, Munich, 1990.
293. L. A. Utracki, *J. Rheol.* **35**, 1615 (1991).
294. J. F. Palierne, *Rheol. Acta* **29**, 204 (1990).
295. R. Muller, in G. O. Shonaike and G. P. Simon, eds., *Polymer Blends and Alloys*, Marcel Dekker, Inc., New York, 1999, Chap. 16.
296. M. Bousmina, J. F. Palierne, and L. A. Utracki, *Polym. Eng. Sci.* **39**, 1049 (1999).
297. M. Iza, M. Bousmina, and R. Jérôme, *Rheol. Acta* **40**, 10 (2001).
298. P. K. Han and J. L. White, *Rubber Chem. Technol.* **68**, 728 (1995).
299. Z. Kruliš and I. Fortelný, *Eur. Polym. J.* **33**, 513 (1997).
300. M. A. López-Manchado and M. Arroyo, *Rubber Chem. Technol.* **74**, 211 (2001).
301. P. M. Subramanian and I. G. Plotzker, in D. R. Paul and C. B. Buckmall, eds., *Polymer Blends*, John Wiley & Sons, Inc., New York, 1999, p. 359.
302. H. B. Hopfenberg and D. R. Paul, in D. R. Paul, and S. Newman, eds., *Polymer Blends*, Academic Press Inc., New York, 1978, p. 445.
303. J. S. Chiou and D. R. Paul, *J. Appl. Polym. Sci.* **33**, 2935 (1987).
304. C. K. Kim, M. A. Vega, and D. R. Paul, *J. Polym. Sci., Part B: Polym. Phys.* **30**, 1131 (1992).
305. T. F. Blahovici and G. R. Brown, *Polym. Eng. Sci.* **27**, 1611 (1988).
306. Y. Nir, M. Narkis, and A. Siegmann, *Polym. Networks Blends* **7**, 139 (1998).
307. J. B. Faisant, A. Ait-Kadi, M. Bousmina, and L. Deschenes, *Polymer* **39**, 533 (1998).
308. J. Kolařík, L. Fambri, A. Pegoretti, and A. Penati, *Polym. Eng. Sci.* **40**, 127 (2000).
309. L. A. Utracki, *Polymer Alloys and Blends, Thermodynamic and Rheology*, Carl Hanser-Verlag, Munich, 1989, p. 10.
310. L. A. Utracki, *Encyclopaedic Dictionary of Commercial Polymer Blends*, Chem Tec Publishing, Toronto, Canada, 1994.

311. L. A. Utracki, *Commercial Polymer Blends*, Chapman & Hall, London, 1998.
312. S. Datta, D. J. Lohse, *Polymeric Compatibilizers*, Carl Hanser-Verlag, Munich 1996.
313. W. E. Baker, C. Scott, and G. H. Hu, eds., *Reactive Polymer Blending*, Carl Hanser-Verlag, Munich 2001.
314. A. H. Hogt, J. Meijer, and J. Jelenič, in S. Al-Malaika, ed., *Reactive Modifiers for Polymers* Chapman & Hall, London, 1997, p. 84.
315. Utracki, *Encyclopaedic Dictionary of Commercial Polymer Blends*, ChemTec Publishing, Toronto, pp. 183–189, 1994.
316. S. Datta and D. J. Lhose, *Polymeric Compatibilizers*, Carl Hanser-Verlag, Munich, 1996, pp. 315–321.
317. M. van Duin and R. J. M. Borggreve, in S. Al-Malaika, ed., *Reactive Modifiers for Polymers*, Chapman & Hall, London, p. 133, 1997.
318. J. Scheirs, *Polymer Recycling*, John Wiley & Sons, Inc., New York, 1998.
319. R. J. Ehrig, ed., *Plastic Recycling*, Carl Hanser-Verlag, Munich, 1989.
320. I. Fortelný, D. Michálková, and Z. Kruliš, *Polym. Degrad. Stab.* **85**, 975 (2004).

## GENERAL REFERENCES

P. J. Flory, *Principles of Polymer Chemistry*, Cornell University Press, Ithaca, N.Y., 1953.
G. L. Lewis and M. Randall, *Thermodynamics*, McGraw-Hill, New York, 1961.
B. D. Gesner, *Encyclopedia of Polymer Science and Technology*, Vol. **10**, Wiley-Interscience, New York, 1969.
J. A. Manson and L. H. Sperling, *Polymer Blends and Composites*, Plenum Press, New York, 1976.
C. B. Bucknall, *Toughened Plastics*, Applied Science Publishers, London, 1977.
R. D. Deanin, in H. F. Mark, N. G. Gaylord, and N. M. Bikales, eds., *Encyclopedia of Polymer Science and Technology*, Supple. Vol. 2, Wiley-Interscience, New York, 1977.
D. R. Paul and S. Newman, eds., *Polymer Blends*, Vols. I, II, Academic Press, Inc., New York, 1978.
O. Olabisi, L. Robeson, and M. T. Shaw, *Polymer—Polymer Miscibility*, Academic Press, Inc., New York, 1979.
L. Sperling, *Interpenetrating Polymer Networks and Related Materials*, Plenum Press, New York, 1981.
D. R. Paul, J. W. Barlow, and H. Keskula, in J. I. Kroschwitz, Ed.-in-ch., *Encyclopedia of Polymer Science and Engineering*, 2nd edition, John Wiley & Sons, New York, 1985.
L. A. Utracki, *Polymer Alloys and Blends*, Hanser Publishers, Munich, 1990.
I. C. Sanchez, *Physics of Polymer Surfaces and Interfaces*, Butterworth-Heiemann, Boston, Mass., 1992.
M. J. Folkes and P. S. Hope, *Polymer Blends and Alloys*, Chapman & Hall, Cambridge, U.K., 1993.
L. A. Utracki, *Encyclopaedic Dictionary of Commercial Polymer Blends*, ChemTec Publishing, Toronto, 1994.
S. Datta and D. J. Lhose, *Polymeric Compatibilizers*, Carl Hanser-Verlag, Munich, 1996.
L. H. Sperling, *Polymeric Multicomponent Materials*, John Wiley & Sons, Inc., New York, 1997.
S. Malaika, *Reactive Modifiers for Polymers*, Chapman & Hall, London, 1997.
L. A. Utracki, *Commercial Polymer Blends*, Chapman & Hall, London, 1998.
G. O. Shonaike and G. P. Simon, *Polymer Blends and Alloys*, Marcel Dekker, Inc., New York, 1999.
D. R. Paul and C. B. Bucknall, eds., *Polymer Blends*, Vols. 1 and 2, John Wiley & Sons, Inc., New York, 2000.

W. E. Baker, C. E. Scott, and G-H. Hu, *Reactive Polymer Blending*, Carl Hanser-Verlag, Munich, 2001.
W. Grellmann, S. Seidler, eds., *Deformation and Fracture Behaviour of Polymers*. Springer-Verlag, Berlin, 2001.
C. Vasile and A. K. Kulshreshtha, eds., *Handbook of Polymer Blends*, Vol. 3A, Rapra, Shawbury, 2003.
C. Vasile and A. K. Kulshreshtha, eds., *Handbook of Polymer Blends*, Vol. 3B, Rapra, Shawbury, 2003.
C. Vasile and A. K. Kulshreshtha, eds., *Handbook of Polymer Blends*, Vol. 4A, Rapra, Shawbury, 2003.
C. Vasile and A. K. Kulshreshtha, eds., *Handbook of Polymer Blends*, Vol. 4B, Rapra, Shawbury, 2003.

ZDENĚK HORÁK
IVAN FORTELNÝ
JAN KOLAŘÍK
DRAHOMÍRA HLAVATÁ
ANTONÍN SIKORA
Institute of Macromolecular Chemistry,
Academy of Sciences of the Czech Republic